

Electronic Supporting Information

Drastic Substituent Effect on the Emission Properties of Quinone diimine Models and Valuable Insight on the Excited States of Emeraldine

Mohammed Abdelhameed, Adam Langlois, Daniel Fortin, Paul-Ludovic Karsenti, Pierre D. Harvey

Table of Content

Experimental section and Materials	2
Instruments and Femtosecond transient absorption spectroscopy	3
Crystallography	4
Fig. S1. Atom numbering for 3 .	4
Fig. S2. Two ORTEP representations of 3 .	5
Table S1. Crystal data and structure refinement for 3 .	5
Table S2. Atomic coordinates and equivalent isotropic displacement parameters for 3 .	6
Table S3. Bond lengths [Å] and angles [°] for 3 .	7
Table S4. Anisotropic displacement parameters for 3 .	8
Table S5. Hydrogen coordinates and isotropic displacement parameters for 3 .	9
Table S6. Torsion angles [°] for 3 .	10
Calculation procedure	11
Table S7. Energy comparison of the optimized geometries for the conformers of 1 and 2 .	11
Fig. S3. Optimised geometry of trans-2 .	12
Table S8. Relative contributions and energy levels of the MOs for trans-2	12
Fig. S4. Representations of the frontier MOs of trans-2	12
Fig. S5. Bar graph representing the calculated oscillator strength (f) and generated spectrum for trans-2	13
Table S9. Calculated positions, f, and major contributions of the first 100 electronic transitions for trans-2 .	13
Fig. S6. Optimised geometry of trans-2'	16
Table S10. Relative contributions and energy levels of the MOs for trans-2'	16
Fig. S7. Representations of the frontier MOs of trans-2'	16
Fig. S8. Bar graph representing the calculated oscillator strength (f) and generated spectrum for trans-2'	17
Table S11. Calculated positions, f, and major contributions of the first 100 electronic transitions for trans-2'	17
Fig. S9. Optimised geometry of cis-2	20
Table S12. Relative contributions and energy levels of the MOs for cis-2	20
Fig. S10. Representations of the frontier MOs of cis-2	20
Fig. S11. Bar graph representing the calculated oscillator strength (f) and generated spectrum for cis-2	21
Table S13. Calculated positions, f, and major contributions of the first 100 electronic transitions for cis-2	21
Fig. S12. Optimised geometry of 1	24
Table S14. Relative contributions and energy levels of the MOs for 1	24
Fig. S13. Representations of the frontier MOs of 1	24
Fig. S14. Bar graph representing the calculated oscillator strength (f) and generated spectrum for 1	25
Table S15. Calculated positions, f, and major contributions of the first 100 electronic transitions for 1	25
Fig. S15. Optimised geometry of 1'	30
Table S16. Relative contributions and energy levels of the MOs for 1'	30
Fig. S16. Representations of the frontier MOs of 1'	30
Fig. S17. Bar graph representing the calculated oscillator strength (f) and generated spectrum for 1'	31
Table S17. Calculated positions, f, and major contributions of the first 100 electronic transitions for 1'	31
Fig. S18. Top: Fluorescence decay of 1 in 2MeTHF at 77K, lamp profile, and curve fit analysed using a double exponential fit. Middle: residual. Bottom: ESM analysis of the decay curve.	32
Fig. S19. Top: Fluorescence decay of 2 in 2MeTHF at 77K and curve fit analysed using the ESM Middle: residual. Bottom: ESM analysis of the decay curve (Y = SiMe ₃).	33
Fig. S20. Top: Phosphorescence decay of 2 in 2MeTHF at 77K, lamp profile analysed using the ESM. Middle: residual. Bottom: ESM analysis of the decay curve (Y = SiMe ₃).	34

Experimental section.

Materials. 4-((Trimethylsilyl)ethynyl)aniline, TiCl₄, 4-dimethylaminopyridine di-*tert*-butyl dicarbonate, triethylamine and 1,4-benzoquinone were purchased from Aldrich and were used without further purification. All solvent were dried prior to be used.

Compound 1. An amount of 1.33 g (7 mmol) of 4-((trimethylsilyl)ethynyl)aniline was dissolved in chlorobenzene and placed in a three-necked round bottomed flask, 1.4 mL (10 mmol) of triethylamine, and 0.16 ml (1.5 mmol) of TiCl₄ were added to the flask using a syringe. A 108.1 mg quantity (1 mmol) of 1,4-benzoquinone was dissolved in a minimum amount of chlorobenzene and added dropwise to the solution. The solution was stirred at 60 °C for 10 h. The mixture was left to cool to room temperature, filtered, and washed with warm chlorobenzene twice. The solution was evaporated. The solid was dissolved in CH₂Cl₂, washed three times with water, dried with MgSO₄, and filtered. The product was purified on a silica column with CH₂Cl₂/Hexanes (1:2) as the eluent to give the desired compound. Yield: 580 mg (70%). IR (KBr)/cm⁻¹ v: 3297 (N-H), 2155 (C≡C), 1593 (C=N). ¹H NMR (400 MHz, CD₂Cl₂): 8.30 (2 H, s), 7.44 (8 H, d), 6.95 (8 H, d), 6.24 (2 H, s), 0.25 (36 H, d), m/z (EI): calculated for C₅₀H₅₆N₄Si₄⁺ : 825.36, Found: 825.36 (M⁺).

Compound 2. To a solution of **1** (1.11 g, 1.35 mmol) in THF (40 ml) under argon at 21°C, was added di-*tert*-butyl dicarbonate, Boc₂O (1.12 g, 5.11 mmol). The solution was cooled on ice bath followed by addition of 4-dimethylaminopyridine, DMAP, (297 mg, 1.36 mmol). The resulting mixture solution was stirred at 21° C for 24 h was evaporated. The crude product was subject to chromatography purification on silica gel, eluent CH₂Cl₂ / hexane (2:1) to give the product as a red solid. Yield: 535 mg (60%). IR (KBr)/cm⁻¹ v: 3303 (N-H), 2161 (C≡C), 1742 (C=O), 1599 (C=N). ¹H NMR (400 MHz, CD₂Cl₂): 7.40 (8 H, dd), 7.16 (4 H, d), 6.77 (2 H, s), 6.68 (4 H, d), 1.40 (18 H, s), 0.25 (36 H, d), m/z (EI): calculated for C₆₀H₇₂N₄O₄Si₄⁺: 1025.46, Found: 1025.24 (M⁺).

Instruments. The ^1H NMR and ^{13}C NMR spectra were collected on a Bruker DRX 300 and 400 spectrometer in deuterated chloroform solution, with tetramethylsilane (TMS) as internal standard. All chemical shifts (δ) and coupling constants (J) are given in ppm and Hertz, respectively. The spectra were measured from freshly prepared samples. The IR spectra were acquired on a Bomem FT-IR MB series spectrometer equipped with a baseline-diffused reflectance. EI-MS were recorded on a LCQ DECA XP Liquid Chromatograph–Mass Spectrometer (Thremo Group). TGA were acquired on a Perkin-Elmer TGA 7 between 50 and 950 °C at 3°C/ min under a nitrogen atmosphere. The UV/vis spectra were recorded on a Hewlett-Packard diode array model 8452A at Sherbrooke. The emission and excitation spectra were obtained by using a double monochromator Fluorolog 2 instrument from Spex (Horiba) or a FLS980 spectrometer from Edinburgh Instrument. Fluorescence and phosphorescence lifetimes were measured on a Timemaster Model TM-3/2003 apparatus from PTI or on a FLS980 spectrometer from Edinburgh Instrument. The source of the PTI was a nitrogen laser with a high-resolution dye laser ($\text{fwhm} \approx 1.5 \text{ ns}$), and the fluorescence lifetimes were obtained from high-quality decays and deconvolution or distribution lifetime analysis. The uncertainties were about 40 ps based on multiple measurements although the reliability on the measurements is 100 ps. The sources of the EI spectrometer was an EPL picosecond diode lasers operating at 375 nm ($\text{FWHM} = 90 \text{ ps}$). The phosphorescence lifetimes were performed on a PTI LS-100 using a 1 μs tungsten flash lamp ($\text{fwhm} \sim 1 \text{ } \mu\text{s}$).

Femtosecond transient absorption spectroscopy.

The fs transient spectra and decay profiles were acquired on an homemade system using a Spitfire sapphire laser from Spectra Physics ($\lambda_{\text{exc}} = 398 \text{ nm}$; $\text{FWHM} = 75 \text{ ps}$; pulse energy = 0.1 $\mu\text{J}/\text{pulse}$, rep. rate = 1 kHz; spot size $\sim 500 \text{ } \mu\text{m}$), an OPA (company) allowing an adjustable excitation from 200 to 3000nm, and a custom made CCD camera of 64 x 1024 pixels sensitive between 200 and 1100 nm. The delay line permitted to probe up to 4 ns with an accuracy of ~ 4 fs. The results were analysed with the program Glotaran (<http://glotaran.org>) permitting to extract a sum of independent exponentials ($I(\lambda, t) = C_1(\lambda) \cdot \exp(-t/\tau_1) + C_2(\lambda) \cdot \exp(-t/\tau_2) + \dots$).

Crystallography: The crystal was grown by slow evaporation of a CH₂Cl₂/toluene (3/1) solution at room temperature. One single crystal was mounted using a glass fiber on the goniometer. Data were collected on an Enraf-Nonius CAD-4 automatic diffractometer at the Université de Sherbrooke using omega scans at 293(2) K. The DIFRAC⁽¹⁾ program was used for centering, indexing, and data collection. Two standard reflections were measured every 100 reflections, no significant intensity decay was observed during data collection. The data were corrected for absorption by empirical methods based on psi scans and reduced with the NRCVAX⁽²⁾ programs. They were solved using SHELXS-97⁽³⁾ and refined by full-matrix least squares on F² with SHELXL-97⁽⁴⁾. The non-hydrogen atoms were refined anisotropically. The hydrogen atoms were placed at idealized calculated geometric position and refined isotropically using a riding model.

- (1) H.D. Flack, E. Blanc and D. Schwarzenbach (1992), *J. Appl. Cryst.*, **25**, 455-459.
- (2) E.J. Gabe, Y. Le Page, J.-P. Charland, F.L. Lee, and P.S. White, (1989) *J. Appl. Cryst.*, **22**, 384-387.
- (3) G. M. Sheldrick, SHELXS-97, G.M. Sheldrick, University of Göttingen, Germany, 1997, Release 97-2.
- (4) G. M. Sheldrick, SHELXL-97, G.M. Sheldrick, University of Göttingen, Germany, 1997, Release 97-2.

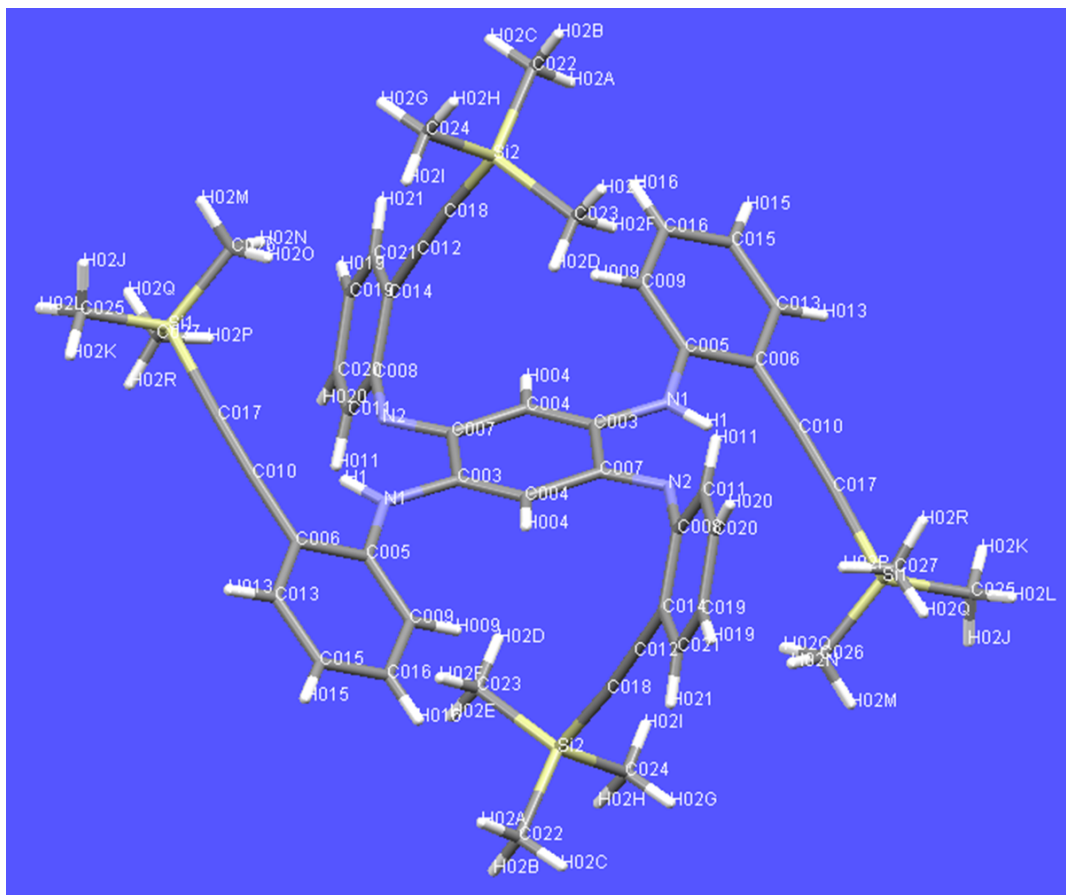


Fig. S1. Atom numbering for 3.

Table S1. Crystal data and structure refinement for **3**.

Empirical formula	C50 H56 N4 Si4	
Formula weight	825.37	
Temperature	293(2) K	
Wavelength	1.54176 Å	
Crystal system	Monoclinic	
Space group	P 21/C	
Unit cell dimensions	a = 13.953(4) Å b = 10.739(4) Å c = 18.125(8) Å	$\alpha = 90^\circ$. $\beta = 105.53(3)^\circ$. $\gamma = 90^\circ$.
Volume	2616.6(17) Å ³	
Z	2	
Density (calculated)	1.048 Mg/m ³	
Absorption coefficient	1.307 mm ⁻¹	
F(000)	880	
Crystal size	0.50 x 0.30 x 0.20 mm ³	
Theta range for data collection	3.29 to 70.02°.	
Index ranges	-17 <= h <= 16, 0 <= k <= 13, 0 <= l <= 22	
Reflections collected	4885	
Independent reflections	4885 [R(int) = 0.0000]	
Completeness to theta = 70.00°	98.6 %	
Refinement method	Full-matrix least-squares on F ²	
Data / restraints / parameters	4885 / 0 / 269	
Goodness-of-fit on F ²	0.952	
Final R indices [I>2sigma(I)]	R1 = 0.1051, wR2 = 0.2971	
R indices (all data)	R1 = 0.2092, wR2 = 0.3591	
Extinction coefficient	0.0044(10)	
Largest diff. peak and hole	0.440 and -0.276 e.Å ⁻³	

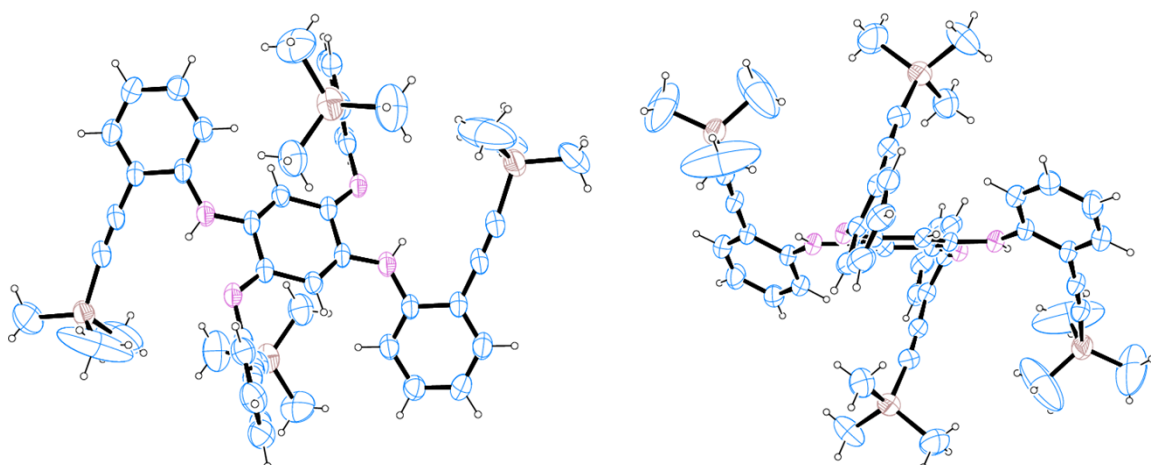


Fig. S2. Two ORTEP representations of **3**. The thermal ellipsoids are at the 30% probability level. The pink, turquoise and brown atoms are respectively N, C and Si. The others are H atoms. **3** is centro-symmetric and the dihedral angles are 70.65 and 39.37° between the plane made by **[Q]** and those made by the -C₆H₄-N= and -C₆H₄-NH- ones, respectively; d(N···H) = 2.161 Å.

Table S2. Atomic coordinates ($x \times 10^4$) and equivalent isotropic displacement parameters ($\text{\AA}^2 \times 10^3$) for **3**. $U(\text{eq})$ is defined as one third of the trace of the orthogonalized U^{ij} tensor.

	x	y	z	$U(\text{eq})$
Si(1)	6090(2)	595(2)	1956(1)	143(1)
Si(2)	8214(2)	-4036(2)	3826(1)	147(1)
N(2)	8051(4)	677(4)	4603(2)	95(1)
N(1)	9154(3)	1578(4)	3789(2)	104(1)
C(003)	9648(5)	799(4)	4367(3)	90(2)
C(004)	10591(4)	485(4)	4538(3)	92(2)
C(005)	9580(4)	2344(5)	3324(3)	99(2)
C(006)	8980(4)	2563(5)	2567(3)	101(2)
C(007)	8953(5)	331(4)	4820(3)	90(2)
C(008)	7372(5)	256(6)	5001(3)	102(2)
C(009)	10466(5)	2912(6)	3593(3)	112(2)
C(010)	8053(5)	1967(6)	2315(3)	107(2)
C(011)	7000(6)	1101(7)	5426(4)	122(2)
C(012)	7384(5)	-1898(6)	4544(3)	109(2)
C(013)	9356(6)	3376(7)	2117(4)	126(2)
C(014)	7026(5)	-957(6)	4961(3)	103(2)
C(015)	10266(7)	3939(7)	2380(4)	137(2)
C(016)	10827(5)	3719(6)	3117(4)	128(2)
C(017)	7286(5)	1432(6)	2131(3)	114(2)
C(018)	7690(5)	-2733(7)	4216(4)	127(2)
C(019)	5979(6)	-420(10)	5778(4)	144(3)
C(020)	6336(7)	767(9)	5829(5)	144(3)
C(021)	6317(6)	-1252(7)	5346(4)	128(2)
C(022)	7851(9)	-5465(8)	4264(8)	232(5)
C(023)	9570(7)	-3841(9)	4114(6)	189(4)
C(024)	7767(10)	-4048(11)	2756(5)	244(6)
C(025)	5323(12)	922(19)	1081(12)	465(19)
C(026)	6307(12)	-968(13)	2108(18)	520(20)
C(027)	5563(12)	1010(30)	2670(14)	580(30)

Table S3. Bond lengths [\AA] and angles [$^\circ$] for **3**.

Si(1)-C(025)	1.695(15)	C(025)-Si(1)-C(027)	111.2(14)
Si(1)-C(027)	1.710(15)	C(025)-Si(1)-C(026)	113.2(11)
Si(1)-C(026)	1.714(14)	C(027)-Si(1)-C(026)	103.1(16)
Si(1)-C(017)	1.847(8)	C(025)-Si(1)-C(017)	112.0(5)
Si(2)-C(018)	1.808(8)	C(027)-Si(1)-C(017)	107.1(5)
Si(2)-C(023)	1.835(10)	C(026)-Si(1)-C(017)	109.7(6)
Si(2)-C(022)	1.859(10)	C(018)-Si(2)-C(023)	107.1(4)
Si(2)-C(024)	1.871(10)	C(018)-Si(2)-C(022)	106.6(4)
N(2)-C(007)	1.269(6)	C(023)-Si(2)-C(022)	110.5(5)
N(2)-C(008)	1.411(8)	C(018)-Si(2)-C(024)	110.7(4)
N(1)-C(003)	1.374(6)	C(023)-Si(2)-C(024)	109.2(5)
N(1)-C(005)	1.417(7)	C(022)-Si(2)-C(024)	112.5(6)
C(003)-C(004)	1.312(7)	C(007)-N(2)-C(008)	119.5(4)
C(003)-C(007)	1.516(8)	C(003)-N(1)-C(005)	127.0(5)
C(004)-C(007) ^{#1}	1.459(7)	C(004)-C(003)-N(1)	127.1(6)
C(005)-C(009)	1.348(8)	C(004)-C(003)-C(007)	122.3(4)
C(005)-C(006)	1.422(7)	N(1)-C(003)-C(007)	110.6(5)
C(006)-C(013)	1.391(8)	C(003)-C(004)-C(007) ^{#1}	122.6(5)
C(006)-C(010)	1.405(9)	C(009)-C(005)-N(1)	122.5(5)
C(007)-C(004) ^{#1}	1.459(7)	C(009)-C(005)-C(006)	121.3(6)
C(008)-C(011)	1.379(9)	N(1)-C(005)-C(006)	115.9(5)
C(008)-C(014)	1.384(9)	C(013)-C(006)-C(010)	123.6(5)
C(009)-C(016)	1.408(9)	C(013)-C(006)-C(005)	117.0(6)
C(010)-C(017)	1.182(8)	C(010)-C(006)-C(005)	119.4(6)
C(011)-C(020)	1.372(10)	N(2)-C(007)-C(004) ^{#1}	127.5(6)
C(012)-C(018)	1.215(9)	N(2)-C(007)-C(003)	117.4(5)
C(012)-C(014)	1.428(9)	C(004) ^{#1} -C(007)-C(003)	115.2(5)
C(013)-C(015)	1.371(9)	C(011)-C(008)-C(014)	118.1(7)
C(014)-C(021)	1.392(9)	C(011)-C(008)-N(2)	118.7(7)
C(015)-C(016)	1.376(9)	C(014)-C(008)-N(2)	123.2(6)
C(019)-C(021)	1.353(10)	C(005)-C(009)-C(016)	120.0(6)
C(019)-C(020)	1.363(11)	C(017)-C(010)-C(006)	177.0(6)
		C(020)-C(011)-C(008)	122.3(8)
		C(018)-C(012)-C(014)	177.1(7)
		C(015)-C(013)-C(006)	122.2(6)
		C(008)-C(014)-C(021)	118.2(7)
		C(008)-C(014)-C(012)	121.8(7)
		C(021)-C(014)-C(012)	120.0(7)
		C(013)-C(015)-C(016)	119.7(7)
		C(015)-C(016)-C(009)	119.8(7)
		C(010)-C(017)-Si(1)	173.7(6)
		C(012)-C(018)-Si(2)	174.0(6)
		C(021)-C(019)-C(020)	118.6(9)
		C(019)-C(020)-C(011)	119.7(8)
		C(019)-C(021)-C(014)	123.0(8)

Symmetry transformations used to generate equivalent atoms: #1 -x+2,-y,-z+1

Table S4. Anisotropic displacement parameters ($\text{\AA}^2 \times 10^3$) for **3**. The anisotropic displacement factor exponent takes the form: $-2\pi^2 [h^2 a^*{}^2 U^{11} + \dots + 2 h k a^* b^* U^{12}]$

	U ¹¹	U ²²	U ³³	U ²³	U ¹³	U ¹²
Si(1)	125(2)	144(2)	135(2)	17(1)	-10(1)	-4(1)
Si(2)	164(2)	120(2)	141(2)	-16(1)	12(2)	25(1)
N(2)	104(3)	91(3)	76(2)	8(2)	-3(2)	6(3)
N(1)	107(3)	106(3)	83(3)	11(2)	-3(2)	7(3)
C(003)	106(4)	78(3)	67(3)	4(2)	-8(3)	10(3)
C(004)	97(4)	87(3)	77(3)	-1(2)	0(3)	-3(3)
C(005)	105(4)	93(3)	82(3)	11(3)	-5(3)	11(3)
C(006)	111(4)	97(4)	78(3)	8(3)	-1(3)	14(3)
C(007)	104(4)	78(3)	73(3)	-2(2)	-2(3)	12(3)
C(008)	105(4)	102(4)	80(3)	-4(3)	-7(3)	9(4)
C(009)	116(5)	103(4)	96(4)	6(3)	-6(3)	1(4)
C(010)	104(4)	116(4)	81(3)	8(3)	-9(3)	13(4)
C(011)	121(5)	128(5)	104(4)	-16(4)	11(4)	-1(5)
C(012)	115(5)	102(4)	95(4)	2(4)	1(3)	-5(4)
C(013)	141(6)	126(5)	95(4)	21(4)	5(4)	8(5)
C(014)	104(4)	111(5)	85(4)	5(3)	7(3)	5(4)
C(015)	155(7)	140(6)	108(5)	39(4)	24(5)	4(5)
C(016)	132(5)	112(5)	123(5)	15(4)	7(4)	-8(4)
C(017)	112(5)	120(5)	93(4)	5(3)	-5(4)	18(4)
C(018)	137(6)	106(5)	118(5)	-13(4)	1(4)	8(4)
C(019)	143(7)	181(8)	107(5)	-19(6)	32(5)	-4(6)
C(020)	134(6)	166(8)	121(6)	-31(5)	17(5)	14(6)
C(021)	128(6)	136(6)	106(5)	17(5)	6(4)	-6(5)
C(022)	267(13)	115(6)	327(15)	20(8)	103(12)	21(7)
C(023)	185(9)	175(8)	188(9)	9(7)	21(7)	42(7)
C(024)	317(16)	227(11)	158(8)	-58(8)	13(9)	68(11)
C(025)	254(15)	550(30)	430(30)	240(20)	-187(16)	-240(20)
C(026)	207(15)	213(15)	1070(70)	210(30)	50(30)	-26(12)
C(027)	310(20)	880(60)	670(50)	-530(50)	330(30)	-350(30)

Table S5. Hydrogen coordinates ($\times 10^4$) and isotropic displacement parameters ($\text{\AA}^2 \times 10^3$) for **3**.

	x	y	z	U(eq)
H(1)	8517	1604	3699	125
H(004)	10984	796	4239	110
H(009)	10840	2771	4094	134
H(011)	7206	1926	5440	146
H(013)	8978	3543	1620	151
H(015)	10503	4467	2061	164
H(016)	11443	4103	3300	153
H(019)	5512	-653	6034	173
H(020)	6131	1348	6135	172
H(021)	6064	-2058	5305	154
H(02A)	8131	-5439	4808	348
H(02B)	8096	-6185	4058	348
H(02C)	7139	-5508	4150	348
H(02D)	9740	-3049	3938	283
H(02E)	9873	-4495	3894	283
H(02F)	9807	-3878	4662	283
H(02G)	7055	-4116	2602	366
H(02H)	8053	-4745	2560	366
H(02I)	7964	-3289	2557	366
H(02J)	5204	177	777	697
H(02K)	5627	1537	833	697
H(02L)	4703	1236	1138	697
H(02M)	5780	-1432	1770	780
H(02N)	6332	-1165	2629	780
H(02O)	6929	-1181	2009	780
H(02P)	5973	721	3152	871
H(02Q)	4914	642	2575	871
H(02R)	5506	1900	2682	871

Table S6. Torsion angles [°] for **3**.

C(005)-N(1)-C(003)-C(004)	-9.6(8)
C(005)-N(1)-C(003)-C(007)	169.4(5)
N(1)-C(003)-C(004)-C(007)#1	178.5(4)
C(007)-C(003)-C(004)-C(007)#1	-0.3(8)
C(003)-N(1)-C(005)-C(009)	-35.4(9)
C(003)-N(1)-C(005)-C(006)	149.6(5)
C(009)-C(005)-C(006)-C(013)	0.9(9)
N(1)-C(005)-C(006)-C(013)	176.0(5)
C(009)-C(005)-C(006)-C(010)	-178.9(6)
N(1)-C(005)-C(006)-C(010)	-3.7(8)
C(008)-N(2)-C(007)-C(004)#1	-0.1(8)
C(008)-N(2)-C(007)-C(003)	179.3(5)
C(004)-C(003)-C(007)-N(2)	-179.2(5)
N(1)-C(003)-C(007)-N(2)	1.8(6)
C(004)-C(003)-C(007)-C(004)#1	0.3(7)
N(1)-C(003)-C(007)-C(004)#1	-178.7(4)
C(007)-N(2)-C(008)-C(011)	110.9(6)
C(007)-N(2)-C(008)-C(014)	-71.9(6)
N(1)-C(005)-C(009)-C(016)	-176.4(6)
C(006)-C(005)-C(009)-C(016)	-1.6(9)
C(013)-C(006)-C(010)-C(017)	167(14)
C(005)-C(006)-C(010)-C(017)	-13(14)
C(014)-C(008)-C(011)-C(020)	2.6(9)
N(2)-C(008)-C(011)-C(020)	179.9(6)
C(010)-C(006)-C(013)-C(015)	-179.8(7)
C(005)-C(006)-C(013)-C(015)	0.5(10)
C(011)-C(008)-C(014)-C(021)	0.5(8)
N(2)-C(008)-C(014)-C(021)	-176.7(5)
C(011)-C(008)-C(014)-C(012)	-178.9(5)
N(2)-C(008)-C(014)-C(012)	3.9(8)
C(018)-C(012)-C(014)-C(008)	138(14)
C(018)-C(012)-C(014)-C(021)	-42(14)
C(006)-C(013)-C(015)-C(016)	-1.1(11)
C(013)-C(015)-C(016)-C(009)	0.4(11)
C(005)-C(009)-C(016)-C(015)	0.9(10)
C(006)-C(010)-C(017)-Si(1)	40(18)
C(025)-Si(1)-C(017)-C(010)	150(5)
C(027)-Si(1)-C(017)-C(010)	28(6)
C(026)-Si(1)-C(017)-C(010)	-84(6)
C(014)-C(012)-C(018)-Si(2)	-32(19)
C(023)-Si(2)-C(018)-C(012)	-62(7)
C(022)-Si(2)-C(018)-C(012)	56(7)
C(024)-Si(2)-C(018)-C(012)	179(100)
C(021)-C(019)-C(020)-C(011)	2.1(12)
C(008)-C(011)-C(020)-C(019)	-4.0(11)
C(020)-C(019)-C(021)-C(014)	1.1(11)
C(008)-C(014)-C(021)-C(019)	-2.4(9)
C(012)-C(014)-C(021)-C(019)	177.1(6)

Symmetry transformations used to generate equivalent atoms: #1 -x+2,-y,-z+1

Calculation procedure:

All density functional theory (DFT) and time dependent density functional theory (TD-DFT) calculations were performed with Gaussian 09 [1] at the Université de Sherbrooke with the Mammouth supercomputer supported by *Le Réseau Québécois De Calculs Hautes Performances*. The DFT geometry optimisations as well as TD-DFT calculations [2-11] were carried out using the B3LYP method. A 6-31g* basis set was used for all atoms [12-17]. The calculated absorption spectra were obtained from GaussSum 2.1 [18]. Second derivative tests were carried out to determine the nature of the stationary points by performing a frequency calculation on each of the optimised geometries. All of the structures presented here show no imaginary frequencies indicating that they all of the geometries are at real energetic minima.

1. Frisch MJ *et al.* *Gaussian, Inc., Wallingford CT*, 2004.
2. Hohenberg P and Kohn W. *Phys. Rev.* 1964; **136**: B864.
3. Hohenberg P and Kohn W. *J. Phys. Rev.* 1965; **140**: A1133.
4. Parr RG and Yang W. *Density-functional theory of atoms and molecules*, Oxford Univ. Press: Oxford, 1989.
5. Salahub DR and Zerner MC. *The Challenge of d and f Electrons, Amer. Chem. Soc. Washington, D.C.* 1989.
6. Bauernschmitt R and Ahlrichs R. *Chem. Phys. Lett.* 1996; **256**: 454.
7. Casida ME, Jamorski C, Casida KC and Salahub DR. *J. Chem. Phys.* 1998; **108**: 4439.
8. Stratmann RE, Scuseria GE and Frisch MJ. *J. Chem. Phys.* 1998; **109**: 8218.
9. Lee C, Yang W and Parr RG. *Phys. Rev. B* 1988; **37**: 785.
10. Miehlich B, Savin A, Stoll H and Preuss H. *Chem. Phys. Lett.* 1989; **157**: 200.
11. Becke AD. *J. Chem. Phys.* 1993; **98**: 5648.
12. Binkley JS, Pople JA and Hehre WJ. *J. Am. Chem. Soc.* 1980; **102**: 939.
13. Gordon MS, Binkley JS, Pople JA, Pietro WJ and Hehre WJ. *J. Am. Chem. Soc.* 1982; **104**: 2797.
14. Pietro WJ, Franci MM, Hehre WJ, Defrees DJ, Pople JA and Binkley JS. *J. Am. Chem. Soc.* 1982; **104**: 5039.
15. Dobbs KD and Hehre WJ. *J. Comput. Chem.* 1986; **7**: 359.
16. Dobbs KD and Hehre WJ. *J. Comput. Chem.* 1987; **8**: 861.
17. Dobbs KD and Hehre WJ. *J. Comput. Chem.* 1987; **8**: 880.
18. O'Boyle NM, Tenderholt AL and Langner KM. *J. Comp. Chem.* 2008; **29**: 839.

Table S7. Energy comparison of the optimized geometries for the conformers of **1** and **2**.

Structure	Energy (Hartree)	Δ (eV; kJmol ⁻¹)	Δ (cm ⁻¹)
trans-2	-4007.60517772		0
trans-2'	-4007.60219001	0.0813; 7.84	655.7
cis-2	-4007.60055178	0.1259; 12.1	1015.3
1	-3315.98838696		0
1'	-3315.98816926	0.0059; 0.57	47.8

The table above shows the energies of each of the investigated conformers. Note that the energy difference between conformations is set to 0 with respect to the lowest energy one. Other conformers certainly exist but an exhaustive analysis will not change the conclusion.

trans-2

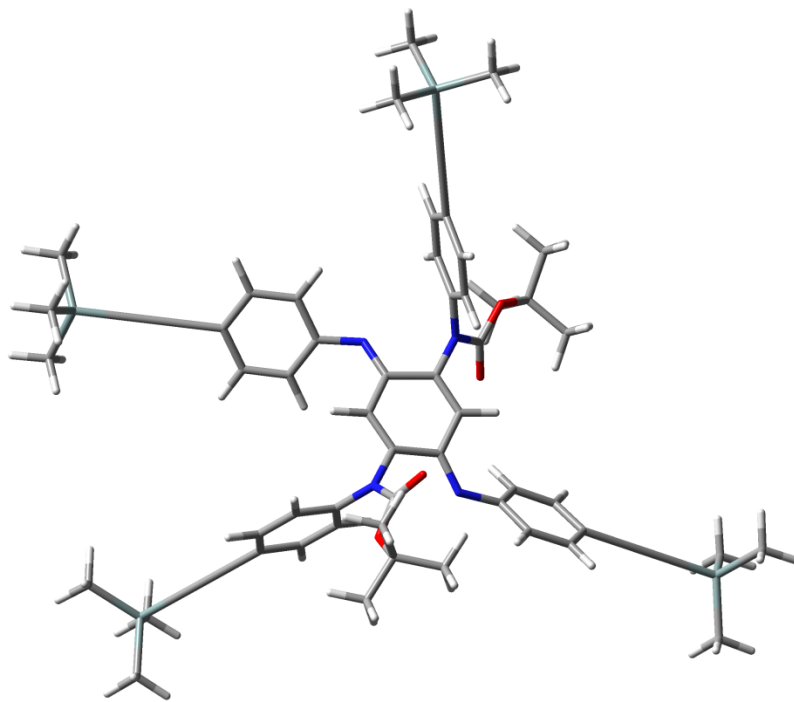


Fig. S3. Optimised geometry of *trans*-**2**.

Table S8. Relative contributions and energy levels (in a.u., gaz phase) of the MOs for *trans*-**2** ($\mathbf{R} = \text{CO}(\text{OCMe}_3)$).

	H-4	H-3	H-2	H-1	HOMO	LUMO	L+1	L+2	L+3	L+4
Energy	-0.2542	-0.2253	-0.2237	-0.2183	-0.2086	-0.1138	-0.0463	-0.0429	-0.0422	-0.0277
$\text{C}_6\text{H}_4\text{C}\equiv\text{CSiMe}_3$	15.6	41.1	28.3	9.6	57.2	24.3	12.3	44.7	24.8	81.3
$\text{NRC}_6\text{H}_2\text{C}\equiv\text{CSiMe}_3$	39.8	39.3	56.3	76.6	8.4	5.6	74.6	43.2	64.9	3.1
$\text{N}=\text{C}_6\text{H}_4=\text{N}, [\mathbf{Q}]$	44.6	19.7	15.5	13.8	34.4	70.2	13.1	12.1	10.3	15.6
Total	100	100	100	100	100	100	100	100	100	100

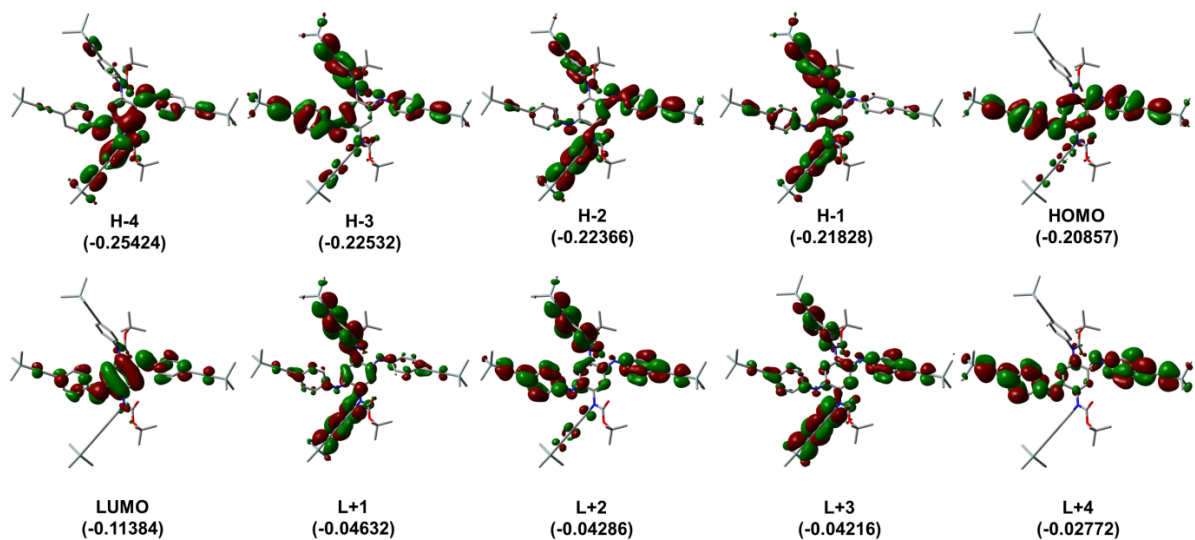


Fig. S4. Representations of the frontier MOs of *trans*-**2**.

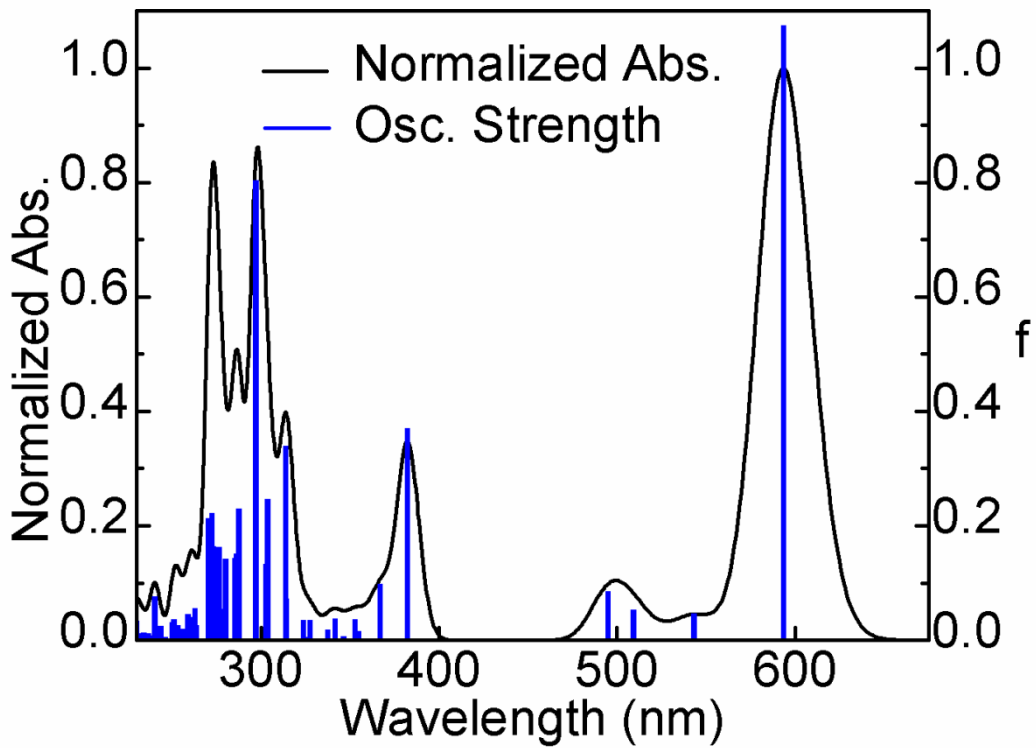


Fig. S5. Bar graph representing the calculated oscillator strength (f , blue) and generated spectrum (black) by assigning 1000 cm^{-1} for each transition (vibronic contributions excluded) for ***trans*-2**.

Table S9. Calculated positions, f , and major contributions of the first 100 electronic transitions for ***trans*-2**.

No.	Wavelength (nm)	Osc. Strength	Major contributors (%)
1	593.3	1.0748	HOMO→LUMO (94%)
2	543.2	0.0469	H-1→LUMO (96%)
3	509.1	0.0523	H-2→LUMO (95%)
4	494.9	0.0848	H-3→LUMO (94%)
5	382.1	0.3703	H-14→LUMO (10%), H-5→LUMO (10%), H-4→LUMO (72%)
6	366.8	0.0983	H-5→LUMO (83%)
7	356.4	0.0028	H-7→LUMO (34%), H-6→LUMO (56%)
8	354.7	0.0151	H-8→LUMO (17%), H-7→LUMO (57%), H-6→LUMO (19%)
9	352.8	0.0361	H-8→LUMO (62%), H-6→LUMO (17%)
10	346.3	0.0062	H-9→LUMO (86%)
11	341.6	0.0374	H-18→LUMO (10%), H-15→LUMO (21%), H-14→LUMO (38%)
12	337.5	0.0181	H-16→LUMO (11%), H-15→LUMO (41%), H-11→LUMO (22%)
13	335.6	0.0002	H-12→LUMO (89%)
14	334.5	0.0029	H-15→LUMO (16%), H-11→LUMO (74%)
15	328.7	0.0028	H-10→LUMO (88%)
16	327.5	0.0346	H-16→LUMO (50%), H-13→LUMO (29%)
17	326.0	0.0057	H-16→LUMO (24%), H-13→LUMO (67%)
18	323.8	0.0352	H-18→LUMO (42%), H-17→LUMO (43%)

19	314.4	0.0724	HOMO→L+1 (93%)
20	313.9	0.3389	H-18→LUMO (26%), H-17→LUMO (44%), H-14→LUMO (13%)
21	303.7	0.2462	HOMO→L+2 (89%)
22	302.8	0.1335	HOMO→L+3 (82%)
23	297.0	0.8041	H-1→L+1 (78%), HOMO→L+3 (10%)
24	287.5	0.2299	H-19→LUMO (20%), H-2→L+1 (12%), H-1→L+2 (27%), H-1→L+3 (14%)
25	286.1	0.1506	H-19→LUMO (26%), H-1→L+2 (50%)
26	285.4	0.1435	H-19→LUMO (17%), H-1→L+3 (51%)
27	280.1	0.1422	H-3→L+1 (31%), H-2→L+1 (38%), HOMO→L+5 (12%)
28	278.8	0.0202	H-19→LUMO (11%), H-2→L+1 (27%), HOMO→L+5 (33%)
29	277.4	0.0544	H-3→L+1 (39%), H-2→L+2 (17%), H-1→L+3 (12%)
30	276.4	0.1626	H-20→LUMO (14%), H-2→L+2 (14%), H-2→L+3 (17%), HOMO→L+5 (25%)
31	274.8	0.0825	H-21→LUMO (18%), H-20→LUMO (62%), H-2→L+2 (11%)
32	274.5	0.059	H-22→LUMO (12%), H-21→LUMO (32%), H-2→L+2 (28%)
33	273.2	0.1635	H-3→L+2 (61%), H-2→L+3 (15%)
34	272.5	0.2216	H-3→L+2 (18%), H-2→L+3 (23%), HOMO→L+4 (40%)
35	271.4	0.1256	H-3→L+3 (74%)
36	270.4	0.213	H-2→L+2 (11%), H-2→L+3 (21%), HOMO→L+4 (31%)
37	263.4	0.0256	H-22→LUMO (30%), H-1→L+5 (30%)
38	262.8	0.0557	H-22→LUMO (30%), H-1→L+5 (14%)
39	261.8	0.0054	H-1→L+4 (16%), H-1→L+6 (20%), HOMO→L+7 (10%)
40	260.9	0.0395	H-2→L+5 (10%), HOMO→L+7 (23%), HOMO→L+8 (21%)
41	259.7	0.0084	H-23→LUMO (58%)
42	259.3	0.0061	H-1→L+4 (60%)
43	258.9	0.0447	H-1→L+5 (12%), HOMO→L+7 (11%), HOMO→L+8 (24%)
44	257.9	0.0024	H-25→LUMO (31%), H-23→LUMO (17%), H-21→LUMO (16%)
45	257.0	0.0195	H-1→L+5 (17%), HOMO→L+9 (12%)
46	254.2	0.0198	H-24→LUMO (23%), H-3→L+4 (13%), H-2→L+4 (41%)
47	253.2	0.0254	H-24→LUMO (39%), H-3→L+4 (11%), HOMO→L+6 (20%)
48	252.6	0.0009	H-13→L+1 (40%), H-13→L+2 (28%), H-13→L+3 (11%)
49	252.6	0.0247	H-2→L+4 (15%), HOMO→L+6 (45%)
50	252.2	0.0024	H-10→L+1 (39%), H-10→L+3 (45%)
51	251.1	0.036	H-2→L+5 (59%)
52	250.3	0.0023	H-28→LUMO (51%), H-27→LUMO (29%)
53	250.2	0.0104	H-28→LUMO (14%), H-27→LUMO (40%), H-26→LUMO (11%)
54	250.1	0.0311	H-27→LUMO (17%), H-3→L+4 (36%), H-3→L+5 (12%), H-2→L+4 (17%)
55	249.1	0.0002	H-3→L+4 (20%), H-3→L+5 (61%)
56	247.8	0.0001	H-26→LUMO (80%)
57	247.5	0.0001	H-29→LUMO (95%)
58	246.1	0.0054	HOMO→L+8 (17%), HOMO→L+9 (47%)

59	243.6	0.0239	H-4→L+1 (60%)
60	242.1	0.0004	H-30→LUMO (71%)
61	240.4	0.0036	H-11→L+2 (32%), H-11→L+4 (23%)
62	240.2	0.0764	H-5→L+1 (42%), H-5→L+2 (10%), H-4→L+3 (12%)
63	239.9	0.0016	H-12→L+2 (23%), H-12→L+3 (19%), H-12→L+4 (22%)
64	238.8	0.0077	H-1→L+7 (77%), H-1→L+9 (11%)
65	238.4	0.0038	H-4→L+2 (38%), H-4→L+3 (31%)
66	236.8	0.012	H-31→LUMO (27%), H-2→L+8 (15%), H-1→L+8 (15%)
67	236.7	0.0024	H-31→LUMO (42%), H-1→L+8 (12%)
68	235.6	0.005	H-32→LUMO (33%), H-3→L+7 (29%)
69	235.1	0.0009	H-32→LUMO (35%), H-3→L+7 (29%)
70	234.0	0.0125	H-2→L+8 (13%), H-1→L+6 (13%), H-1→L+8 (28%)
71	233.6	0.0072	H-3→L+6 (49%), H-1→L+6 (21%), H-1→L+8 (11%)
72	232.6	0.012	H-5→L+1 (10%), H-4→L+1 (13%), H-4→L+2 (28%), H-4→L+3 (19%)
73	231.1	0.0031	H-2→L+6 (69%), H-1→L+6 (12%)
74	230.8	0.0012	H-3→L+12 (10%), HOMO→L+10 (12%), HOMO→L+12 (20%), HOMO→L+14 (16%)
75	230.4	0.0019	H-33→LUMO (26%), H-2→L+7 (24%)
76	230.3	0.0005	H-2→L+7 (19%), HOMO→L+12 (25%)
77	230.0	0.0133	H-5→L+1 (17%), H-5→L+2 (24%)
78	229.9	0.0336	H-33→LUMO (45%), H-2→L+7 (16%)
79	228.5	0.0079	H-2→L+7 (12%), H-2→L+9 (33%), H-1→L+9 (22%)
80	228.0	0.0056	H-5→L+2 (22%), H-5→L+3 (45%)
81	226.6	0.0024	H-8→L+1 (29%), H-3→L+8 (36%)
82	226.4	0.0022	H-2→L+13 (26%), H-1→L+13 (25%)
83	226.3	0.0057	H-8→L+1 (31%), H-3→L+8 (28%)
84	225.8	0.0013	H-3→L+11 (25%), H-2→L+11 (11%), H-1→L+11 (45%)
85	225.5	0.0006	H-6→L+1 (24%), H-6→L+2 (26%), H-6→L+3 (18%)
86	225.0	0.0045	H-3→L+9 (50%)
87	223.8	0.0031	H-7→L+1 (77%)
88	222.7	0.0265	H-6→L+1 (14%), HOMO→L+10 (18%)
89	222.4	0.0335	H-9→L+1 (16%), H-6→L+2 (14%)
90	222.2	0.0036	H-34→LUMO (61%)
91	222.2	0.0056	H-34→LUMO (26%), H-9→L+1 (22%), H-9→L+2 (10%)
92	222.0	0.0015	H-8→L+2 (19%), H-8→L+3 (46%)
93	221.3	0.0114	H-6→L+2 (11%), H-4→L+4 (33%)
94	220.8	0.0043	H-35→LUMO (79%)
95	220.5	0.0388	H-9→L+2 (12%), H-4→L+5 (23%)
96	220.3	0.0386	H-16→L+1 (22%), H-9→L+2 (10%), H-4→L+5 (24%)
97	220.0	0.0056	H-11→L+1 (44%)
98	219.9	0.0276	H-14→L+1 (12%), H-11→L+1 (15%)
99	219.8	0.0358	H-16→L+1 (17%), H-11→L+1 (11%), H-9→L+3 (10%)
100	218.9	0.0249	H-7→L+2 (25%), H-7→L+3 (13%)

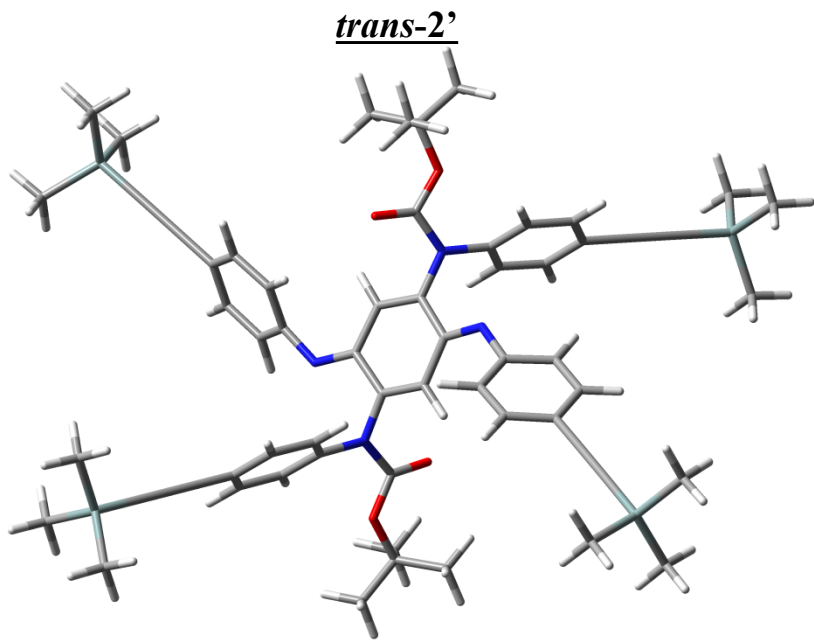


Fig. S6. Optimised geometry of *trans*-2'.

Table S10. Relative contributions and energy levels (in a.u., gaz phase) of the MOs for *trans*-2' ($\text{R} = \text{CO}(\text{OCMe}_3)$).

	H-4	H-3	H-2	H-1	HOMO	LUMO	L+1	L+2	L+3	L+4
Energy	-0.2544	-0.2261	-0.2224	-0.2165	-0.2081	-0.1164	-0.0463	-0.0435	-0.0397	-0.0289
$\text{C}_6\text{H}_4\text{C}\equiv\text{CSiMe}_3$	11.2	48.7	12.9	16.2	55.9	23.6	2.3	55.8	25.1	79.7
$\text{NRC}_6\text{H}_2\text{C}\equiv\text{CSiMe}_3$	47.3	31.8	74.7	68.3	9.5	4.6	79.6	31.2	67.5	4.2
$\text{N}=\text{C}_6\text{H}_4=\text{N}, [\text{Q}]$	41.5	19.5	12.4	15.4	34.6	71.8	18.1	13.0	7.4	16.1
Total	100	100	100	100	100	100	100	100	100	100

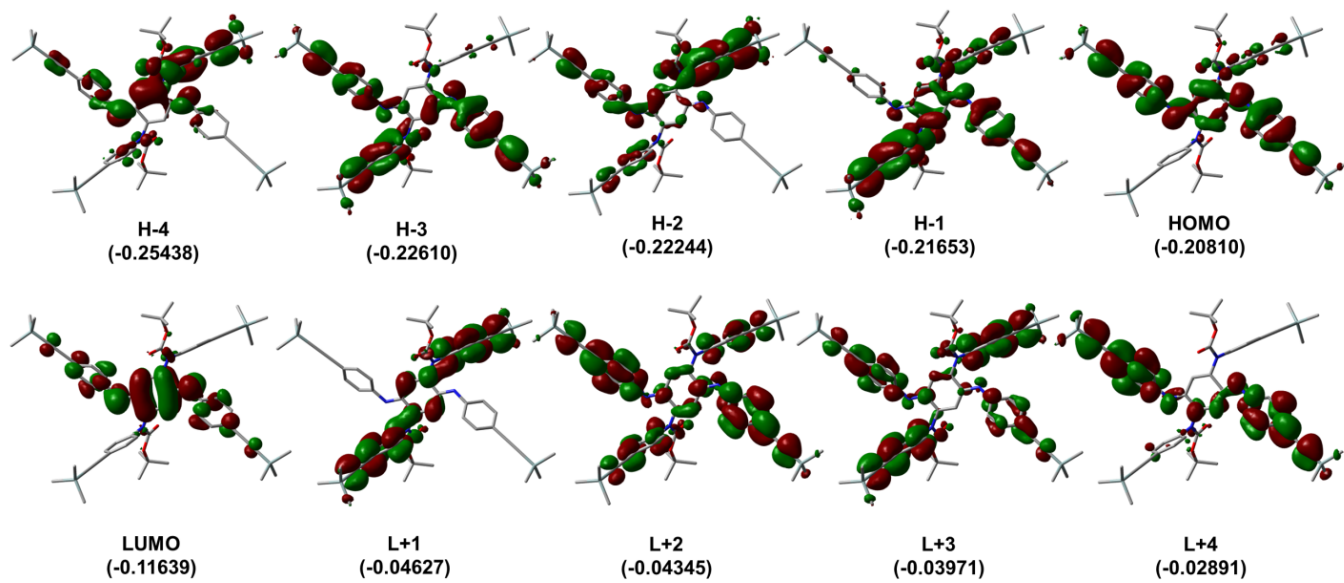


Fig. S7. Representations of the frontier MOs of *trans*-2'.

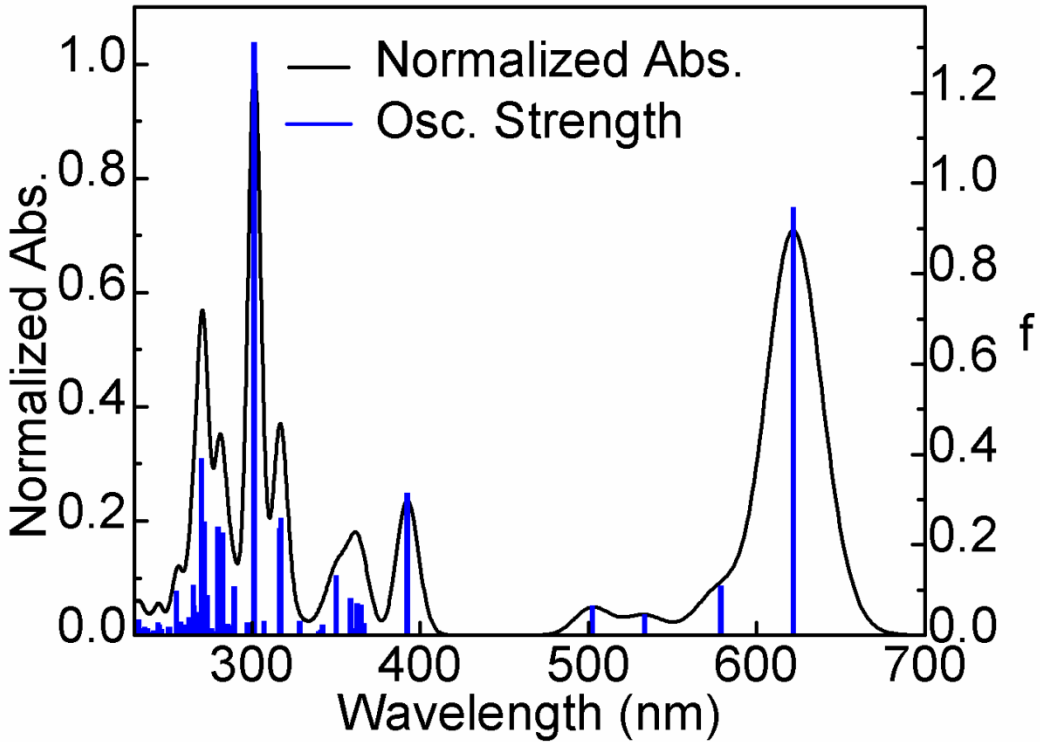


Fig. S8. Bar graph representing the calculated oscillator strength (f , blue) and generated spectrum (black) by assigning 1000 cm^{-1} for each transition (vibronic contributions excluded) for ***trans-2'***.

Table S11. Calculated positions, f , and major contributions of the first 100 electronic transitions for ***trans-2'***.

No.	Wavelength (nm)	Osc. Strength	Major contributors (%)
1	621.8	0.9467	HOMO→LUMO (95%)
2	578.5	0.1084	H-1→LUMO (96%)
3	533.3	0.0465	H-2→LUMO (97%)
4	502.3	0.0647	H-3→LUMO (96%)
5	392.2	0.3147	H-4→LUMO (80%)
6	366.7	0.0268	H-6→LUMO (37%), H-5→LUMO (55%)
7	364.9	0.0666	H-7→LUMO (76%), H-6→LUMO (15%)
8	362.5	0.0706	H-9→LUMO (20%), H-8→LUMO (22%), H-6→LUMO (25%), H-5→LUMO (16%)
9	360.9	0.0149	H-9→LUMO (24%), H-8→LUMO (65%)
10	358.6	0.0816	H-15→LUMO (12%), H-9→LUMO (47%), H-5→LUMO (12%)
11	350.0	0.1326	H-15→LUMO (10%), H-14→LUMO (72%)
12	342.0	0.0222	H-15→LUMO (14%), H-12→LUMO (58%)
13	341.2	0.0117	H-15→LUMO (16%), H-13→LUMO (12%), H-12→LUMO (37%)
14	339.7	0.0088	H-15→LUMO (12%), H-13→LUMO (76%)
15	336.4	0.0027	H-16→LUMO (21%), H-10→LUMO (66%)
16	335.1	0.0004	H-11→LUMO (89%)
17	333.7	0.0006	H-16→LUMO (54%), H-15→LUMO (12%), H-10→LUMO (23%)

18	328.3	0.0313	H-18→LUMO (15%), H-17→LUMO (73%)
19	317.2	0.2591	H-18→LUMO (41%), H-17→LUMO (12%), HOMO→L+1 (24%)
20	316.2	0.2362	H-18→LUMO (14%), HOMO→L+1 (71%)
21	307.2	0.0311	HOMO→L+2 (89%)
22	301.3	1.3118	H-1→L+1 (81%)
23	297.4	0.0277	HOMO→L+3 (90%)
24	289.5	0.1076	H-2→L+1 (18%), H-1→L+2 (64%)
25	287.4	0.0208	H-29→LUMO (14%), H-19→LUMO (33%), H-1→L+2 (19%)
26	285.6	0.0251	H-2→L+1 (28%), H-1→L+3 (34%)
27	282.6	0.2269	H-3→L+1 (20%), H-2→L+1 (32%), H-1→L+3 (30%)
28	281.2	0.0048	H-20→LUMO (81%), H-19→LUMO (18%)
29	279.7	0.24	H-2→L+2 (43%), HOMO→L+4 (19%), HOMO→L+5 (17%)
30	278.5	0.0077	H-21→LUMO (93%)
31	277.5	0.0042	H-2→L+2 (42%), HOMO→L+4 (16%), HOMO→L+5 (23%)
32	276.1	0.0147	H-3→L+1 (55%), H-1→L+3 (22%), HOMO→L+5 (10%)
33	273.2	0.0878	H-3→L+2 (13%), HOMO→L+4 (44%), HOMO→L+5 (28%)
34	271.5	0.2506	H-3→L+2 (62%), H-2→L+3 (11%)
35	270.1	0.3903	H-2→L+3 (71%)
36	266.8	0.0499	H-3→L+3 (15%), H-1→L+4 (33%), H-1→L+5 (23%)
37	265.5	0.0644	H-23→LUMO (14%), H-22→LUMO (19%), H-3→L+3 (28%), H-1→L+4 (16%)
38	265.2	0.1109	H-22→LUMO (45%), H-3→L+3 (35%)
39	264.9	0.0166	H-23→LUMO (58%), H-22→LUMO (17%)
40	262.6	0.0391	H-1→L+4 (10%), HOMO→L+6 (33%)
41	261.9	0.002	H-29→LUMO (24%), H-19→LUMO (14%)
42	261.5	0.0007	HOMO→L+7 (40%)
43	260.3	0.0122	H-1→L+4 (20%), H-1→L+5 (21%), H-1→L+8 (10%), HOMO→L+6 (11%)
44	259.4	0.0235	H-2→L+5 (12%), HOMO→L+8 (11%)
45	257.6	0.029	H-24→LUMO (49%)
46	256.4	0.0172	H-2→L+4 (28%), H-1→L+5 (14%), H-1→L+8 (10%)
47	255.2	0.0973	H-24→LUMO (19%), H-2→L+4 (40%)
48	253.7	0.0003	H-28→LUMO (16%), H-27→LUMO (70%)
49	253.2	0.0002	H-29→LUMO (12%), H-28→LUMO (74%)
50	252.5	0.0007	H-26→LUMO (23%), H-11→L+1 (35%), H-11→L+2 (10%), H-11→L+3 (19%)
51	252.5	0.0001	H-25→LUMO (46%), H-10→L+1 (21%), H-10→L+3 (13%)
52	251.5	0.0003	H-25→LUMO (42%), H-10→L+1 (25%), H-10→L+3 (15%)
53	251.3	0.0004	H-26→LUMO (65%), H-11→L+1 (14%)
54	251.1	0.0175	H-3→L+4 (57%), H-2→L+4 (11%), H-2→L+5 (11%)
55	250.6	0.0173	H-3→L+4 (13%), H-2→L+5 (54%)
56	249.1	0.002	HOMO→L+8 (73%)
57	246.2	0.0128	H-3→L+5 (40%), HOMO→L+9 (25%)
58	245.1	0.0032	H-3→L+5 (41%), HOMO→L+9 (25%)

59	244.7	0.022	H-30→LUMO (54%), H-4→L+1 (12%)
60	244.1	0.0283	H-30→LUMO (13%), H-4→L+1 (56%)
61	241.5	0.0091	H-1→L+6 (57%), HOMO→L+6 (13%)
62	241.1	0.0049	H-31→LUMO (76%)
63	241.0	0.0006	H-13→L+2 (42%), H-13→L+3 (10%), H-13→L+4 (23%)
64	239.9	0.0027	H-32→LUMO (77%)
65	239.7	0.0009	H-12→L+2 (38%), H-12→L+3 (16%), H-12→L+4 (28%)
66	239.6	0.0069	H-1→L+7 (70%)
67	238.0	0.0149	H-4→L+2 (69%)
68	236.4	0.0179	H-6→L+1 (30%), H-5→L+1 (24%)
69	235.0	0.0007	H-3→L+7 (10%), H-2→L+6 (16%), H-2→L+7 (30%)
70	233.9	0.0033	H-33→LUMO (19%), H-2→L+6 (28%), H-1→L+8 (10%), H-1→L+9 (16%)
71	233.3	0.0148	H-4→L+3 (53%)
72	232.9	0.0095	H-4→L+3 (14%), H-3→L+6 (25%), H-1→L+6 (10%)
73	232.8	0.0338	H-33→LUMO (56%)
74	231.4	0.0046	H-3→L+6 (17%), H-2→L+6 (31%), H-2→L+9 (11%), H-1→L+9 (15%)
75	231.3	0.0009	HOMO→L+10 (12%), HOMO→L+11 (28%)
76	230.8	0.0008	HOMO→L+10 (11%), HOMO→L+11 (28%)
77	228.7	0.0288	H-5→L+1 (10%), H-3→L+8 (27%), H-1→L+8 (18%), H-1→L+9 (18%)
78	227.8	0.0034	H-5→L+2 (11%), H-3→L+7 (36%), H-2→L+7 (23%)
79	227.3	0.0278	H-5→L+2 (48%), H-3→L+7 (13%)
80	227.0	0.0043	H-3→L+13 (13%), H-1→L+13 (40%), H-1→L+14 (14%)
81	226.9	0.0057	H-2→L+8 (44%), H-2→L+9 (17%)
82	226.4	0.0042	H-2→L+12 (32%)
83	226.3	0.0064	H-9→L+1 (15%), H-8→L+1 (33%)
84	225.9	0.0027	H-9→L+1 (38%), H-8→L+1 (25%)
85	225.5	0.0071	H-8→L+1 (10%), H-6→L+2 (47%)
86	224.8	0.0108	H-7→L+2 (55%)
87	224.5	0.006	H-9→L+1 (17%)
88	224.3	0.0005	H-34→LUMO (93%)
89	224.1	0.0215	H-14→L+1 (12%), H-7→L+1 (15%), H-5→L+1 (16%), H-3→L+8 (14%)
90	223.5	0.005	H-35→LUMO (20%), H-3→L+9 (36%)
91	223.3	0.001	H-35→LUMO (70%), H-3→L+9 (12%)
92	222.9	0.0115	H-15→L+1 (11%), H-7→L+1 (18%), H-6→L+1 (14%)
93	222.2	0.0062	HOMO→L+10 (31%), HOMO→L+14 (15%)
94	221.8	0.0056	H-7→L+3 (10%), H-6→L+3 (11%), H-4→L+4 (19%)
95	221.8	0.0097	H-4→L+4 (43%)
96	220.1	0.0598	H-15→L+2 (13%), H-6→L+3 (12%)
97	219.6	0.0011	H-17→L+1 (15%), H-15→L+1 (26%), H-14→L+1 (22%)
98	218.9	0.0238	H-9→L+2 (26%), H-4→L+5 (14%)
99	218.8	0.018	H-14→L+2 (14%), H-8→L+2 (38%)
100	218.6	0.0251	H-13→L+1 (16%), H-9→L+2 (14%), H-8→L+2 (11%), H-7→L+3 (13%)

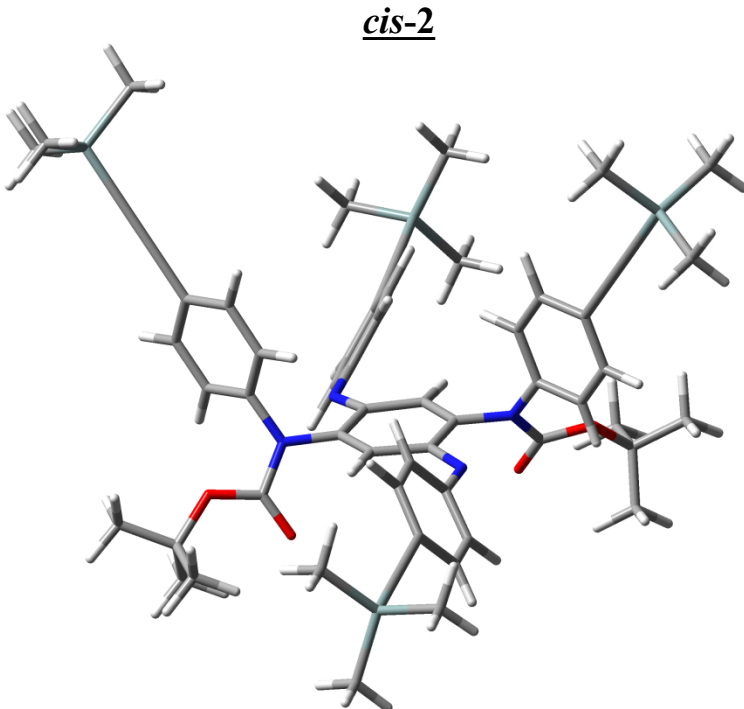


Fig. S9. Optimised geometry of *cis*-2. Note, attempts to calculate another conformer (like *trans*-2') with a different g led to *cis*-2 systematically. Steric hindrance drives this effect.

Table S12. Relative contributions and energy levels (in a.u., gaz phase) of the MOs for *cis*-2 (**R** = CO(OCMe₃)).

Energy	H-4	H-3	H-2	H-1	HOMO	LUMO	L+1	L+2	L+3	L+4
C ₆ H ₄ C≡CSiMe ₃	2.0	52.4	0.6	19.6	61.3	21.9	5.2	0.3	78.0	82.0
NRC ₆ H ₂ C≡CSiMe ₃	74.8	26.5	91.8	62.4	4.6	4.5	76.4	97.5	5.8	4.0
N=C ₆ H ₄ =N, [Q]	23.2	21.2	7.6	18.0	34.1	73.6	18.4	2.2	16.2	14.0
Total	100	100	100	100	100	100	100	100	100	100

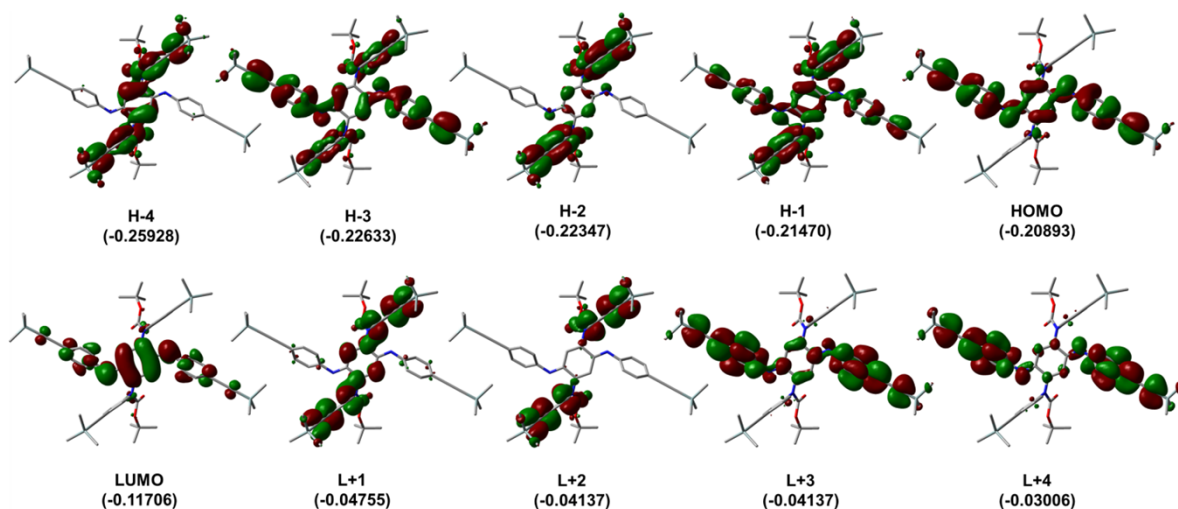


Fig. S10. Representations of the frontier MOs of *cis*-2.

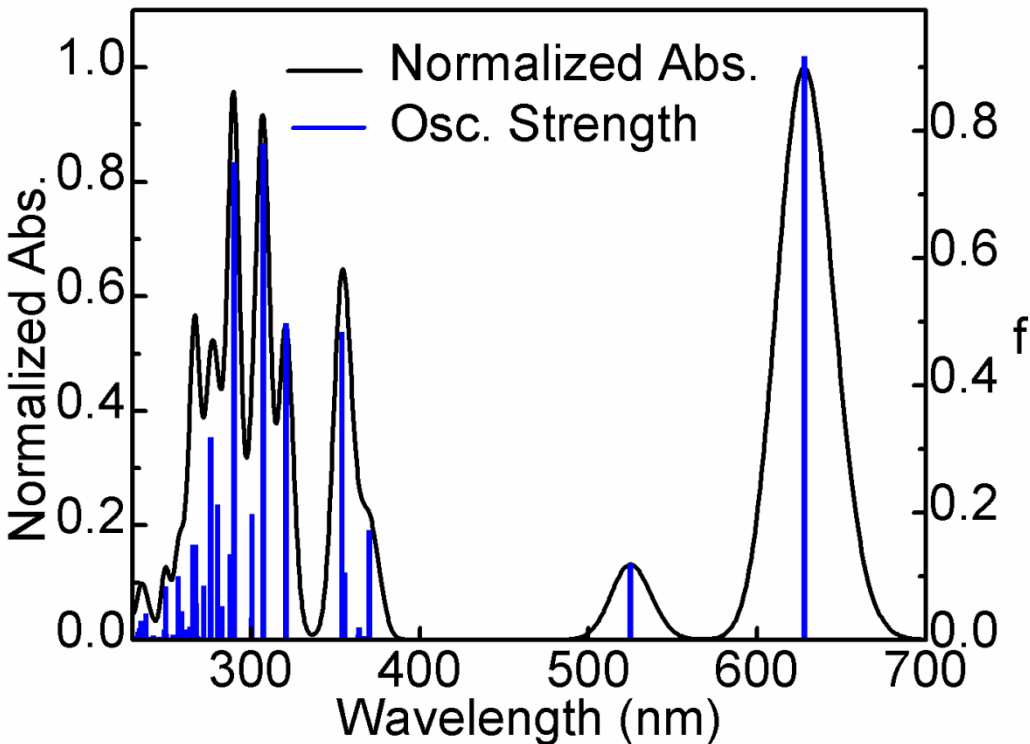


Fig. S11. Bar graph representing the calculated oscillator strength (f , blue) and generated spectrum (black) by assigning 1000 cm^{-1} for each transition (vibronic contributions excluded) for *cis*-2.

Table S13. Calculated positions, f , and major contributions of the first 100 electronic transitions for *cis*-2.

No.	Wavelength (nm)	Osc. Strength	Major contributors (%)
1	627.9	0.9172	HOMO→LUMO (96%)
2	607.4	0.0033	H-1→LUMO (98%)
3	524.9	0.1205	H-2→LUMO (97%)
4	507.4	0.0022	H-3→LUMO (96%)
5	378.6	0.0015	H-4→LUMO (96%)
6	370.1	0.1721	H-14→LUMO (12%), H-6→LUMO (77%)
7	367.3	0.0055	H-7→LUMO (93%)
8	364.0	0.0196	H-9→LUMO (94%)
9	363.3	0.0082	H-8→LUMO (94%)
10	355.4	0.1062	H-16→LUMO (10%), H-14→LUMO (10%), H-6→LUMO (13%), H-5→LUMO (59%)
11	353.7	0.4839	H-14→LUMO (65%), H-5→LUMO (14%)
12	342.4	0.0001	H-15→LUMO (13%), H-12→LUMO (37%), H-11→LUMO (39%)
13	342.0	0.0031	H-13→LUMO (27%), H-10→LUMO (63%)
14	341.5	0.0011	H-15→LUMO (63%), H-12→LUMO (25%)
15	336.5	0.0002	H-13→LUMO (42%), H-10→LUMO (22%)
16	336.4	0.0006	H-17→LUMO (43%), H-13→LUMO (14%), H-11→LUMO (28%)
17	334.6	0.0002	H-17→LUMO (33%), H-15→LUMO (19%), H-12→LUMO (21%), H-11→LUMO

			(24%)
18	332.8	0.0039	H-18→LUMO (38%), H-16→LUMO (36%), H-13→LUMO (12%)
19	320.5	0.4982	H-18→LUMO (43%), H-16→LUMO (35%)
20	317.3	0.001	HOMO→L+1 (95%)
21	307.2	0.7805	H-1→L+1 (87%)
22	300.5	0.1982	H-2→L+1 (10%), H-1→L+2 (10%), HOMO→L+3 (74%)
23	300.4	0.0344	HOMO→L+2 (96%)
24	289.9	0.7504	H-2→L+1 (20%), H-1→L+2 (56%), HOMO→L+3 (18%)
25	287.5	0.135	H-1→L+3 (85%)
26	286.8	0.0031	H-29→LUMO (26%), H-20→LUMO (16%), H-19→LUMO (32%)
27	282.6	0.0527	H-20→LUMO (17%), H-2→L+1 (51%), H-1→L+2 (21%)
28	282.0	0.009	H-20→LUMO (61%), H-19→LUMO (26%)
29	281.6	0.0045	H-21→LUMO (97%)
30	280.1	0.213	H-3→L+1 (84%)
31	275.9	0.3179	H-2→L+2 (19%), HOMO→L+4 (59%)
32	275.2	0.0004	HOMO→L+5 (84%)
33	272.9	0.0018	H-2→L+3 (76%), H-1→L+4 (18%)
34	271.9	0.0852	H-2→L+2 (51%), HOMO→L+4 (19%)
35	268.1	0.0055	H-2→L+3 (18%), H-1→L+4 (68%)
36	267.4	0.0465	H-23→LUMO (26%), H-3→L+2 (50%)
37	267.4	0.0571	H-22→LUMO (42%), H-3→L+3 (35%)
38	267.0	0.1493	H-3→L+3 (28%), H-2→L+2 (19%), H-1→L+5 (37%)
39	266.7	0.0824	H-23→LUMO (47%), H-3→L+2 (35%)
40	265.4	0.1491	H-24→LUMO (15%), H-22→LUMO (34%), H-3→L+3 (14%), H-1→L+5 (16%)
41	263.7	0.0209	H-29→LUMO (40%), H-19→LUMO (31%)
42	262.3	0.0146	H-1→L+7 (12%), HOMO→L+6 (53%)
43	261.3	0.0156	H-1→L+6 (12%), HOMO→L+7 (56%)
44	260.3	0.0159	H-7→L+2 (10%), H-6→L+1 (14%), H-2→L+5 (19%), H-1→L+8 (27%)
45	258.7	0.0454	H-24→LUMO (50%), H-1→L+9 (10%)
46	256.8	0.1003	H-24→LUMO (20%), H-2→L+4 (17%), H-1→L+5 (16%), H-1→L+9 (14%)
47	254.2	0.0003	H-27→LUMO (12%), H-26→LUMO (36%), H-25→LUMO (45%)
48	254.2	0.0002	H-26→LUMO (60%), H-25→LUMO (29%)
49	253.7	0.0081	H-2→L+4 (75%)
50	253.0	0.0001	H-3→L+4 (85%)
51	252.9	0.0004	H-28→LUMO (30%), H-27→LUMO (11%)
52	252.8	0.0003	H-28→LUMO (16%), H-27→LUMO (23%), H-13→L+1 (13%), H-13→L+2 (10%)
53	251.7	0.0007	H-28→LUMO (35%), H-27→LUMO (12%)
54	251.7	0.0005	H-28→LUMO (18%), H-27→LUMO (30%), H-13→L+1 (11%)
55	249.8	0.0095	HOMO→L+8 (85%)
56	249.3	0.084	H-2→L+5 (68%), H-1→L+8 (10%)
57	248.5	0.0164	HOMO→L+9 (85%)
58	246.0	0.0045	H-3→L+5 (82%)
59	245.6	0.0001	H-30→LUMO (78%), H-23→LUMO (14%)

60	242.5	0.0001	H-1→L+6 (76%), HOMO→L+7 (14%)
61	242.1	0.0057	H-1→L+7 (65%), HOMO→L+6 (13%)
62	241.9	0.0075	H-31→LUMO (82%)
63	241.1	0.0047	H-32→LUMO (84%)
64	240.7	0.0004	H-13→L+3 (13%), H-12→L+4 (12%), H-11→L+3 (12%), H-11→L+4 (13%), H-10→L+3 (21%)
65	240.6	0.0007	H-12→L+3 (25%), H-11→L+3 (10%), H-10→L+3 (15%), H-10→L+4 (19%)
66	239.6	0.0053	H-4→L+1 (71%)
67	237.6	0.042	H-5→L+1 (57%), H-4→L+2 (21%)
68	234.9	0.0301	H-33→LUMO (80%)
69	234.4	0.009	H-2→L+9 (14%), H-1→L+8 (49%)
70	234.0	0.018	H-2→L+8 (16%), H-1→L+9 (51%)
71	232.8	0.0131	H-3→L+6 (59%), HOMO→L+7 (12%)
72	232.1	0.002	H-3→L+7 (55%), HOMO→L+6 (10%)
73	231.3	0.0005	H-3→L+11 (15%), H-1→L+11 (11%), HOMO→L+10 (20%), HOMO→L+13 (13%), HOMO→L+14 (23%)
74	231.2	0.0003	H-2→L+6 (78%)
75	231.2	0.0013	H-2→L+6 (12%), HOMO→L+11 (43%)
76	231.0	0.0055	H-14→L+1 (17%), H-5→L+1 (19%), H-4→L+2 (26%)
77	230.6	0.0011	H-2→L+7 (85%)
78	227.6	0	H-9→L+1 (13%), H-5→L+3 (66%)
79	227.4	0.0099	H-8→L+1 (75%)
80	226.9	0.0046	H-9→L+1 (63%)
81	226.7	0.0162	H-6→L+1 (27%), H-5→L+1 (10%), H-4→L+2 (14%)
82	226.7	0.0011	H-2→L+12 (33%), H-1→L+13 (29%)
83	226.6	0.001	H-2→L+13 (23%), H-1→L+12 (29%)
84	225.9	0.0006	H-8→L+1 (13%), H-7→L+1 (11%), H-5→L+2 (34%), H-4→L+3 (15%)
85	225.5	0.0005	H-3→L+8 (53%), H-2→L+9 (21%)
86	225.3	0.0411	H-5→L+2 (14%), H-4→L+3 (47%), H-3→L+9 (20%)
87	225.0	0.0136	H-35→LUMO (35%), H-7→L+1 (26%), H-5→L+2 (11%)
88	224.9	0.0007	H-34→LUMO (93%)
89	224.7	0.0023	H-35→LUMO (58%), H-7→L+1 (16%), H-5→L+2 (10%)
90	224.2	0.0167	H-4→L+3 (29%), H-3→L+9 (49%), H-2→L+8 (14%)
91	224.0	0.002	H-6→L+3 (39%), H-3→L+8 (11%), HOMO→L+10 (10%)
92	222.7	0.0017	H-7→L+3 (78%)
93	222.4	0.0109	H-14→L+1 (36%), H-7→L+2 (17%), H-6→L+1 (20%)
94	222.0	0.0227	H-17→L+1 (15%), H-15→L+1 (33%), H-14→L+2 (17%)
95	221.8	0.0061	H-6→L+3 (29%), HOMO→L+10 (33%), HOMO→L+14 (15%)
96	219.9	0.0002	H-12→L+1 (50%), H-11→L+1 (38%)
97	219.9	0	H-13→L+1 (24%), H-10→L+1 (61%)
98	218.9	0.0125	H-8→L+2 (62%), H-7→L+2 (12%)
99	218.6	0.0086	H-9→L+2 (87%)
100	218.4	0.0356	H-15→L+1 (29%), H-6→L+2 (24%)

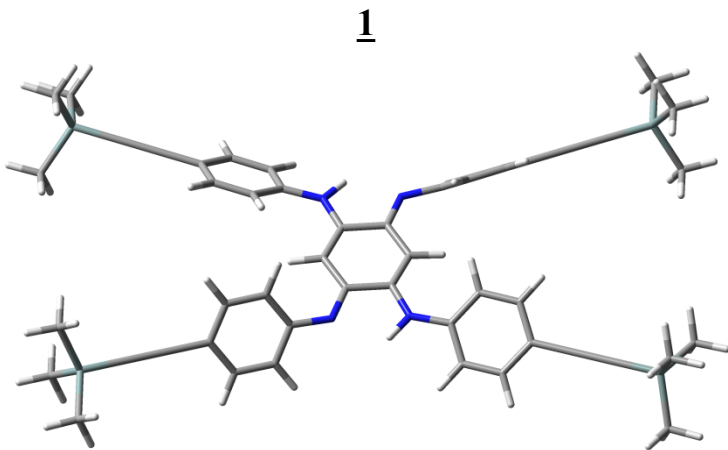


Fig. S12. Optimised geometry of **1**.

Table S14. Relative contributions and energy levels (in a.u., gaz phase) of the MOs for **1** (**R** = H).

	H-4	H-3	H-2	H-1	HOMO	LUMO	L+1	L+2	L+3	L+4
Energy	-0.2465	-0.2248	-0.2162	-0.2034	-0.1957	-0.1031	-0.0438	-0.0384	-0.0328	-0.0249
C ₆ H ₄ C≡CSiMe ₃	1.7	66.2	24.4	39.2	10.9	19.7	4.4	80.2	29.0	53.8
NRC ₆ H ₂ C≡CSiMe ₃	70.8	9.2	60.9	25.1	56.1	16.9	79.6	6.5	66.7	31.0
N=C ₆ H ₄ =N, [Q]	27.5	24.6	14.6	35.7	33.0	63.4	16.1	13.3	4.2	15.2
Total	100	100	100	100	100	100	100	100	100	100

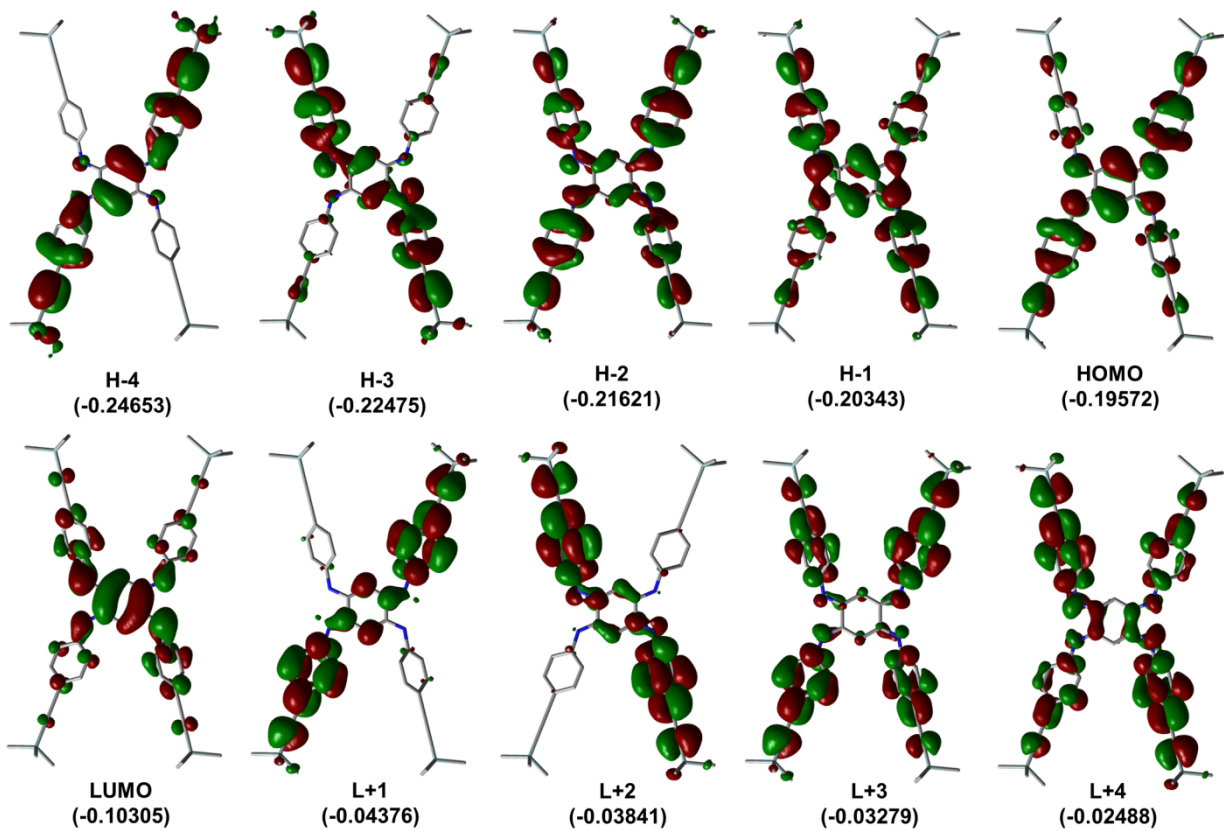


Fig. S13. Representations of the frontier MOs of **1**.

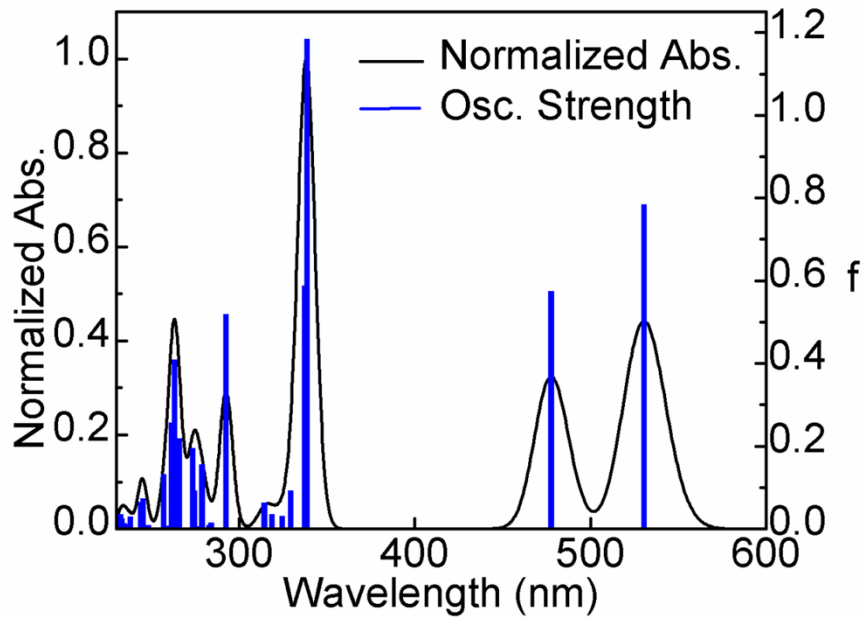


Fig. S14. Bar graph representing the calculated oscillator strength (f , blue) and generated spectrum (black) by assigning 1000 cm^{-1} for each transition (vibronic contributions excluded) for **1**.

Table S15. Calculated positions, f , and major contributions of the first 100 electronic transitions for **1**.

No.	Wavelength (nm)	Osc. Strength	Major contributors (%)
1	614.2	0	HOMO→LUMO (99%)
2	530.4	0.7841	H-1→LUMO (93%)
3	477.6	0.5744	H-2→LUMO (94%)
4	443.7	0.0008	H-3→LUMO (94%)
5	363.9	0.0001	H-4→LUMO (95%)
6	338.6	1.1842	H-5→LUMO (36%), HOMO→L+1 (56%)
7	337.2	0.5885	H-5→LUMO (41%), HOMO→L+1 (36%)
8	330.1	0.0032	H-6→LUMO (96%)
9	329.4	0.093	H-7→LUMO (86%)
10	324.6	0.0316	H-14→LUMO (11%), HOMO→L+2 (74%)
11	318.6	0.0351	H-14→LUMO (10%), H-12→LUMO (61%)
12	318.0	0.0016	H-13→LUMO (11%), H-1→L+1 (74%)
13	317.0	0	H-13→LUMO (74%), H-1→L+1 (12%)
14	314.3	0.0624	H-14→LUMO (56%), H-12→LUMO (17%)
15	311.9	0.0001	H-9→LUMO (40%), H-8→LUMO (52%)
16	311.6	0.0023	H-9→LUMO (51%), H-8→LUMO (39%)
17	308.8	0.002	H-15→LUMO (35%), H-1→L+2 (44%)
18	307.0	0	H-11→LUMO (87%)
19	307.0	0.0003	H-12→LUMO (13%), H-10→LUMO (83%)
20	305.7	0.0012	H-15→LUMO (21%), HOMO→L+3 (64%)

21	301.5	0.0008	H-15→LUMO (28%), H-1→L+2 (19%), HOMO→L+3 (27%), HOMO→L+4 (11%)
22	292.8	0.0001	HOMO→L+4 (82%)
23	292.4	0.5187	H-1→L+3 (94%)
24	287.8	0.001	H-2→L+1 (83%), H-2→L+2 (10%)
25	284.1	0.0146	HOMO→L+5 (76%)
26	283.0	0.0094	H-1→L+5 (10%), HOMO→L+6 (75%)
27	278.9	0.1558	H-16→LUMO (24%), H-1→L+4 (57%)
28	275.9	0.0061	H-2→L+2 (69%), HOMO→L+8 (13%)
29	274.4	0.0919	H-3→L+1 (79%)
30	274.3	0.0162	H-1→L+8 (13%), HOMO→L+7 (70%)
31	273.6	0.1946	H-16→LUMO (37%), H-3→L+2 (16%), H-1→L+4 (18%)
32	273.2	0.0038	H-2→L+2 (14%), H-1→L+7 (14%), HOMO→L+8 (62%)
33	265.7	0.2183	H-2→L+3 (78%)
34	263.3	0.4093	H-3→L+2 (35%), H-1→L+6 (32%)
35	262.9	0.0012	H-1→L+5 (83%), HOMO→L+6 (13%)
36	261.3	0.2573	H-3→L+2 (16%), H-1→L+6 (51%)
37	259.7	0.0047	H-1→L+7 (62%), HOMO→L+8 (22%)
38	259.4	0.0078	H-1→L+8 (64%), HOMO→L+7 (19%)
39	257.3	0.0001	H-17→LUMO (69%), H-3→L+3 (15%)
40	256.9	0.1323	H-3→L+2 (12%), H-2→L+4 (84%)
41	255.5	0	H-17→LUMO (13%), H-3→L+3 (79%)
42	249.1	0.0002	H-2→L+5 (66%)
43	248.4	0.0086	H-2→L+6 (71%)
44	247.5	0	H-19→LUMO (54%), H-3→L+4 (17%)
45	247.2	0.0003	H-19→LUMO (14%), H-3→L+4 (66%)
46	245.2	0.0731	H-18→LUMO (63%), H-4→L+1 (15%)
47	245.2	0.0018	H-3→L+8 (18%), H-2→L+7 (52%), H-1→L+7 (10%)
48	244.9	0.051	H-4→L+1 (10%), H-3→L+7 (17%), H-2→L+8 (42%), H-1→L+8 (10%)
49	244.4	0.0007	H-11→L+1 (38%), H-10→L+3 (17%)
50	244.3	0.0005	H-11→L+3 (19%), H-10→L+1 (40%)
51	243.8	0.0646	H-18→LUMO (13%), H-4→L+1 (57%), HOMO→L+9 (11%)
52	240.7	0.0001	H-21→LUMO (10%), H-9→L+2 (14%), H-8→L+2 (27%), H-8→L+4 (11%)
53	240.7	0.0004	H-22→LUMO (10%), H-9→L+2 (28%), H-9→L+4 (11%), H-8→L+2 (15%)
54	239.0	0.0009	H-5→L+1 (80%), H-4→L+3 (11%)
55	238.0	0.0292	H-2→L+10 (10%), HOMO→L+9 (30%), HOMO→L+11 (21%)
56	237.3	0.0008	H-2→L+11 (12%), HOMO→L+10 (54%)
57	236.5	0.0108	H-20→LUMO (79%)
58	235.6	0.0079	H-22→LUMO (19%), H-21→LUMO (17%), H-4→L+2 (13%), H-1→L+12 (14%)
59	235.5	0	H-22→LUMO (24%), H-21→LUMO (27%), HOMO→L+12 (12%)
60	235.4	0.0027	H-4→L+2 (81%)
61	234.6	0.0137	H-22→LUMO (20%), H-21→LUMO (20%), HOMO→L+9 (10%)

62	234.5	0.0001	H-22→LUMO (18%), H-21→LUMO (16%), HOMO→L+12 (11%)
63	234.3	0.0002	H-24→LUMO (83%), H-23→LUMO (11%)
64	234.3	0.0004	H-23→LUMO (83%)
65	233.3	0.0007	H-26→LUMO (10%), H-25→LUMO (47%), H-19→LUMO (10%), H-5→L+2 (16%)
66	233.0	0.0242	H-3→L+5 (43%), HOMO→L+9 (16%), HOMO→L+13 (12%)
67	232.7	0.0003	H-25→LUMO (15%), H-5→L+2 (64%)
68	232.5	0.0351	H-3→L+5 (47%), HOMO→L+9 (18%)
69	232.2	0.0001	H-3→L+6 (85%)
70	230.9	0.0021	H-3→L+8 (33%), H-2→L+7 (29%), H-1→L+9 (10%)
71	230.2	0.0021	H-3→L+7 (48%), H-2→L+8 (39%)
72	229.1	0.0001	H-5→L+1 (10%), H-4→L+3 (52%), H-3→L+8 (10%), H-1→L+9 (11%)
73	228.9	0	H-26→LUMO (41%), H-25→LUMO (19%), H-4→L+3 (11%), H-1→L+9 (11%)
74	226.6	0.0001	H-26→LUMO (27%), H-4→L+3 (13%), H-1→L+9 (39%)
75	224.8	0.0255	H-27→LUMO (58%), H-5→L+3 (10%), HOMO→L+14 (16%)
76	224.4	0.0212	H-5→L+3 (68%)
77	224.1	0.0151	H-6→L+1 (80%)
78	224.0	0.001	H-7→L+1 (71%)
79	223.6	0.0112	H-12→L+1 (22%), H-7→L+1 (24%), H-4→L+6 (18%), H-2→L+5 (10%)
80	223.4	0.0188	H-13→L+1 (27%), H-4→L+5 (23%), H-2→L+6 (12%)
81	221.5	0.0841	H-27→LUMO (14%), H-5→L+4 (14%), HOMO→L+14 (48%)
82	220.0	0.0002	H-4→L+4 (78%)
83	217.7	0.0001	H-1→L+13 (14%), HOMO→L+12 (57%)
84	217.5	0.0001	H-8→L+1 (25%), H-1→L+12 (10%), HOMO→L+11 (10%), HOMO→L+13 (34%)
85	217.4	0	H-9→L+1 (48%), H-8→L+1 (37%)
86	217.4	0.0016	H-9→L+1 (34%), H-8→L+1 (29%), HOMO→L+13 (17%)
87	217.1	0.0005	H-14→L+2 (32%), H-1→L+14 (18%)
88	216.0	0.0002	H-14→L+1 (31%), H-1→L+14 (41%)
89	215.7	0.1303	H-15→L+2 (16%), H-5→L+4 (49%)
90	214.9	0.0038	H-12→L+2 (41%), H-2→L+9 (23%)
91	214.9	0.0019	H-13→L+2 (61%), H-6→L+2 (10%)
92	214.0	0.0103	H-14→L+2 (17%), H-12→L+2 (20%), H-2→L+9 (28%)
93	214.0	0.0024	H-13→L+2 (15%), H-6→L+2 (36%)
94	213.5	0.0003	H-1→L+10 (63%), HOMO→L+11 (23%)
95	213.3	0.0007	H-14→L+1 (12%), H-1→L+11 (34%), H-1→L+13 (10%), HOMO→L+10 (18%)
96	213.0	0.0266	H-7→L+2 (29%)
97	212.8	0.0457	H-14→L+1 (13%), H-7→L+2 (34%), H-2→L+9 (26%)
98	212.1	0.1602	H-15→L+2 (15%), H-6→L+2 (23%)
99	211.5	0.0051	H-13→L+1 (11%), H-11→L+2 (70%)
100	211.4	0.0023	H-12→L+2 (11%), H-10→L+2 (72%)

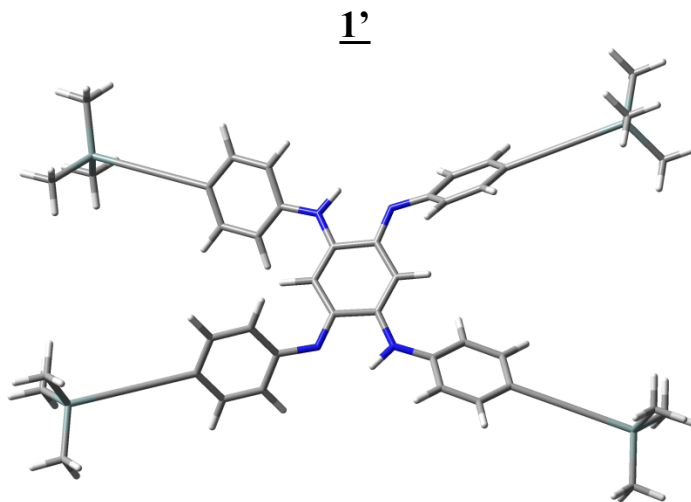


Fig. S15. Optimised geometry of **1'**.

Table S16. Relative contributions and energy levels (in a.u., gaz phase) of the MOs for **1'** (**R** = H).

	H-4	H-3	H-2	H-1	HOMO	LUMO	L+1	L+2	L+3	L+4
Energy	-0.2467	0.22347	0.21922	0.20228	0.19551	0.10252	0.04406	0.03809	-0.0344	-0.0228
C ₆ H ₄ C≡CSiMe ₃	4.3	64.6	30.0	36.5	10.1	19.7	10.6	71.6	32.4	52.6
NRC ₆ H ₂ C≡CSiMe ₃	68.9	10.6	57.4	30.0	58.9	16.6	74.6	10.9	61.8	34.9
N=C ₆ H ₄ =N, [Q]	26.8	24.8	12.6	33.5	31.0	63.6	14.8	17.6	5.9	12.5
Total	100	100	100	100	100	100	100	100	100	100

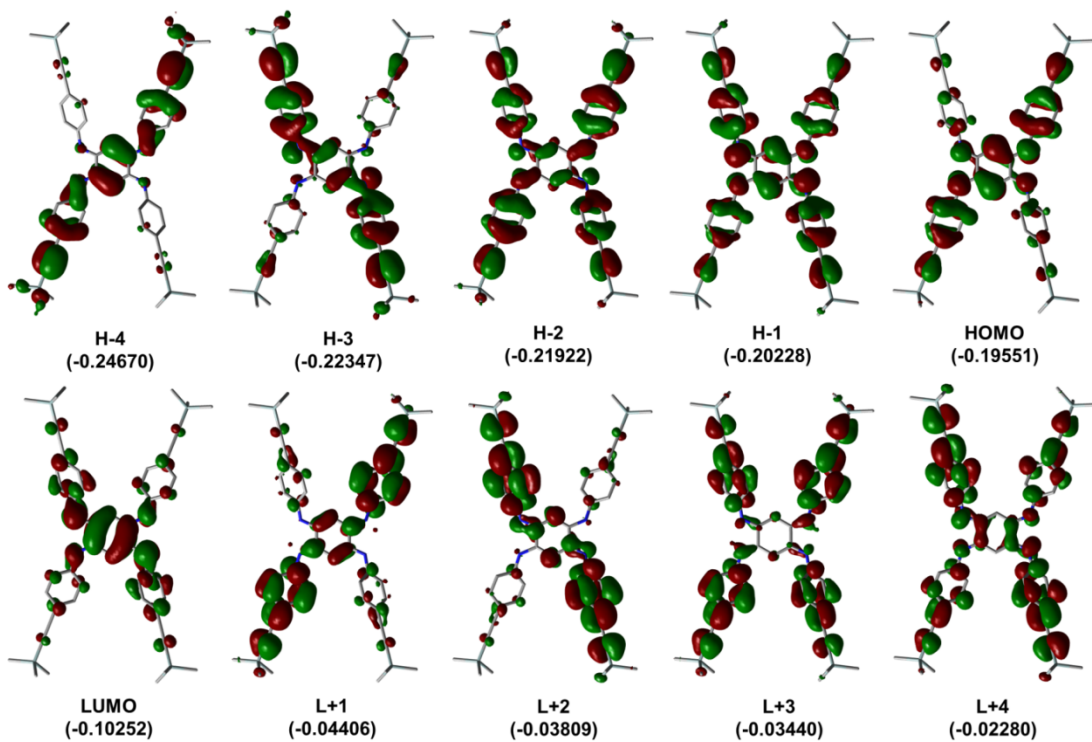


Fig. S16. Representations of the frontier MOs of **1'**.

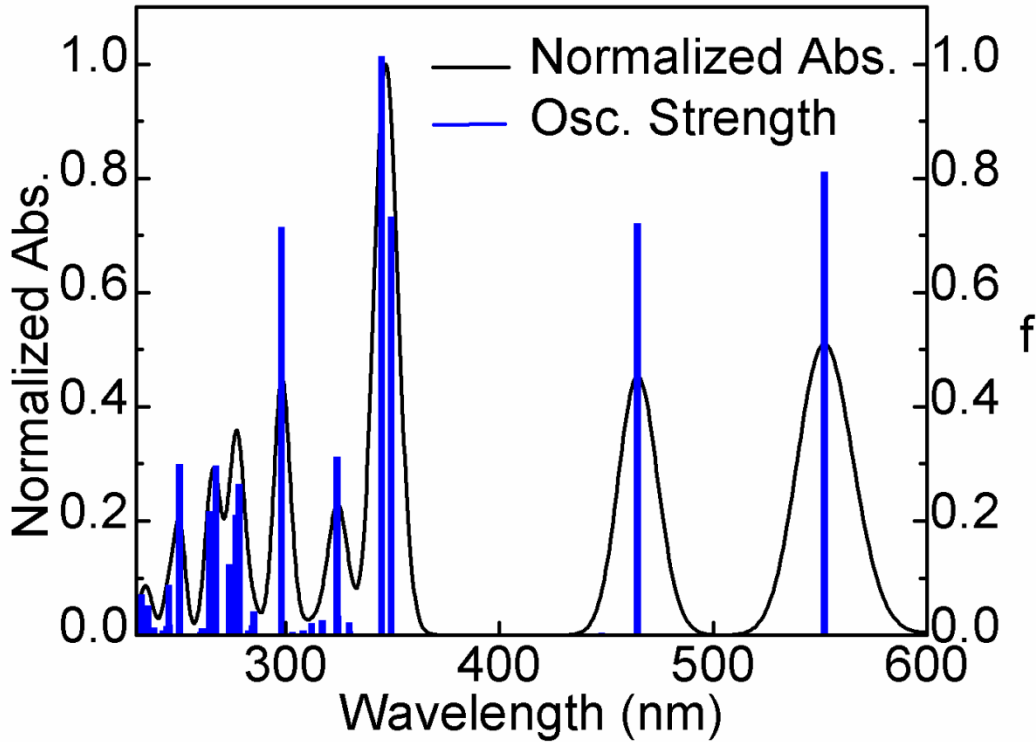


Fig. S17. Bar graph representing the calculated oscillator strength (f , blue) and generated spectrum (black) by assigning 1000 cm^{-1} for each transition (vibronic contributions excluded) for **1'**.

Table S17. Calculated positions, f , and major contributions of the first 100 electronic transitions for **1'**.

No.	Wavelength (nm)	Osc. Strength	Major contributors (%)
1	623.8	0.0176	HOMO->LUMO (99%)
2	552.0	0.8113	H-1->LUMO (97%)
3	464.5	0.7203	H-2->LUMO (97%)
4	447.8	0.0041	H-3->LUMO (96%)
5	363.0	0.0017	H-4->LUMO (97%)
6	349.3	0.733	H-5->LUMO (79%)
7	344.8	1.014	HOMO->L+1 (97%)
8	329.8	0.0071	H-6->LUMO (96%)
9	329.7	0.0214	H-7->LUMO (95%)
10	324.5	0.0335	H-1->L+1 (91%)
11	324.0	0.312	HOMO->L+2 (88%)
12	317.1	0.0254	H-12->LUMO (70%), H-10->LUMO (14%)
13	316.6	0.0003	H-13->LUMO (81%), H-11->LUMO (10%)
14	312.1	0.0207	H-14->LUMO (61%), H-9->LUMO (11%)
15	311.4	0	H-9->LUMO (14%), H-8->LUMO (44%), HOMO->L+3 (28%)
16	310.7	0.0022	H-14->LUMO (14%), H-9->LUMO (59%), H-8->LUMO (21%)
17	310.5	0.0002	H-9->LUMO (10%), H-8->LUMO (26%), HOMO->L+3 (56%)
18	308.2	0.0073	H-15->LUMO (29%), H-1->L+2 (49%)

19	306.1	0.0005	H-12->LUMO (12%), H-10->LUMO (76%)
20	306.0	0.0002	H-11->LUMO (79%)
21	303.1	0.0055	H-15->LUMO (52%), H-1->L+2 (36%)
22	298.1	0.7145	H-1->L+3 (94%)
23	290.1	0.0026	HOMO->L+4 (92%)
24	285.0	0.0411	H-1->L+6 (11%), HOMO->L+5 (77%)
25	284.4	0.0162	H-1->L+5 (12%), HOMO->L+6 (75%)
26	282.7	0.0074	H-2->L+1 (89%)
27	278.2	0.2642	H-16->LUMO (49%), H-3->L+1 (12%), H-1->L+4 (31%)
28	276.8	0.2098	H-3->L+1 (82%), H-1->L+4 (12%)
29	275.1	0.0272	H-2->L+2 (69%), HOMO->L+8 (14%)
30	274.5	0.0094	H-1->L+8 (16%), HOMO->L+7 (71%)
31	273.7	0.1243	H-16->LUMO (24%), H-3->L+2 (24%), H-2->L+3 (10%), H-1->L+4 (32%)
32	273.5	0.0021	H-2->L+2 (17%), H-1->L+7 (16%), HOMO->L+8 (58%)
33	267.3	0.297	H-16->LUMO (13%), H-3->L+2 (37%), H-2->L+3 (15%), H-1->L+4 (18%)
34	264.2	0.2166	H-3->L+2 (27%), H-2->L+3 (66%)
35	263.7	0.001	H-1->L+5 (83%), HOMO->L+6 (16%)
36	263.3	0.0031	H-1->L+6 (81%), HOMO->L+5 (14%)
37	261.0	0.0113	H-3->L+3 (13%), H-1->L+7 (52%), HOMO->L+8 (23%)
38	260.3	0.0009	H-3->L+3 (77%), H-1->L+7 (10%)
39	260.3	0.0058	H-1->L+8 (63%), HOMO->L+7 (21%)
40	257.8	0.0007	H-17->LUMO (85%)
41	250.3	0.2989	H-2->L+4 (92%)
42	247.2	0.0014	H-18->LUMO (15%), H-3->L+4 (64%)
43	246.7	0	H-18->LUMO (55%), H-3->L+4 (12%), H-2->L+5 (10%)
44	245.7	0.0001	H-2->L+5 (51%)
45	245.6	0.0185	H-4->L+1 (14%), H-2->L+6 (51%)
46	245.4	0.088	H-4->L+1 (57%)
47	244.7	0.0006	H-11->L+3 (14%), H-10->L+1 (29%), H-5->L+1 (12%)
48	244.5	0.0149	H-11->L+1 (32%), H-10->L+3 (13%)
49	243.9	0	H-5->L+1 (13%), H-3->L+8 (21%), H-2->L+7 (28%)
50	243.7	0.0019	H-3->L+7 (30%), H-2->L+8 (33%), H-1->L+8 (13%)
51	243.5	0.0019	H-5->L+1 (62%)
52	242.6	0.0079	H-19->LUMO (78%)
53	240.9	0.0001	H-9->L+2 (26%), H-8->L+2 (13%), H-8->L+3 (12%), H-8->L+4 (11%)
54	240.9	0.0003	H-9->L+2 (13%), H-9->L+3 (12%), H-9->L+4 (11%), H-8->L+2 (27%)
55	238.3	0.0123	H-1->L+10 (12%), HOMO->L+9 (30%), HOMO->L+11 (22%)
56	237.7	0.0006	HOMO->L+10 (49%)
57	236.9	0.0015	H-5->L+2 (68%)
58	236.3	0.0135	H-20->LUMO (75%)
59	235.7	0.0519	H-4->L+2 (72%)
60	235.2	0.0092	H-22->LUMO (12%), H-21->LUMO (17%), H-1->L+12 (22%)

61	235.2	0	H-22->LUMO (18%), H-21->LUMO (13%), H-3->L+12 (11%), H-1->L+13 (13%), HOMO->L+12 (16%)
62	234.3	0.012	H-22->LUMO (23%), H-21->LUMO (34%)
63	234.3	0.0008	H-22->LUMO (33%), H-21->LUMO (22%)
64	233.8	0.0007	H-23->LUMO (95%)
65	233.7	0.0005	H-24->LUMO (95%)
66	233.2	0.0027	H-3->L+5 (86%), H-2->L+6 (13%)
67	232.9	0	H-3->L+6 (85%), H-2->L+5 (12%)
68	232.9	0	H-25->LUMO (71%)
69	232.5	0.071	HOMO->L+9 (40%), HOMO->L+13 (20%)
70	230.7	0.0006	H-5->L+2 (11%), H-4->L+3 (72%)
71	229.2	0.0121	H-5->L+3 (77%), H-4->L+2 (12%)
72	229.2	0.0026	H-3->L+8 (21%), H-2->L+7 (36%), H-1->L+9 (18%)
73	228.6	0.0014	H-3->L+7 (39%), H-2->L+8 (55%)
74	228.3	0.0001	H-26->LUMO (34%), H-3->L+8 (14%), H-2->L+7 (15%), H-1->L+9 (15%)
75	226.9	0	H-26->LUMO (37%), H-1->L+9 (37%)
76	224.7	0.094	H-27->LUMO (17%), HOMO->L+14 (56%)
77	224.2	0.0018	H-6->L+1 (86%)
78	224.2	0.0007	H-7->L+1 (89%)
79	223.7	0.0284	H-12->L+1 (30%), H-5->L+5 (12%), H-4->L+6 (20%), H-2->L+5 (16%)
80	223.5	0.1121	H-13->L+1 (30%), H-5->L+6 (11%), H-4->L+5 (21%), H-2->L+6 (17%)
81	221.8	0.0277	H-27->LUMO (56%), H-5->L+4 (13%), HOMO->L+14 (13%)
82	220.2	0.0017	H-14->L+1 (13%), H-14->L+2 (13%), H-4->L+4 (31%), H-1->L+14 (19%)
83	218.1	0.0003	H-1->L+13 (13%), HOMO->L+12 (69%)
84	218.0	0.1163	H-15->L+2 (11%), H-5->L+4 (40%), HOMO->L+13 (12%)
85	217.8	0.0308	H-1->L+12 (13%), HOMO->L+11 (15%), HOMO->L+13 (37%)
86	217.4	0.0005	H-9->L+1 (19%), H-4->L+4 (42%)
87	217.3	0.0011	H-9->L+1 (16%), H-8->L+1 (69%)
88	217.3	0.0002	H-9->L+1 (50%), H-4->L+4 (12%)
89	216.5	0.003	H-14->L+1 (10%), H-1->L+14 (47%)
90	215.8	0.0241	H-6->L+2 (50%), H-5->L+4 (13%), H-3->L+7 (11%)
91	215.3	0.0009	H-13->L+1 (20%), H-13->L+2 (49%)
92	215.2	0.0903	H-12->L+2 (18%), H-7->L+2 (36%), H-3->L+8 (11%)
93	214.9	0.0729	H-12->L+2 (19%), H-7->L+2 (24%)
94	214.5	0.0021	H-1->L+10 (63%), HOMO->L+11 (23%)
95	214.4	0.0114	H-1->L+11 (39%), H-1->L+13 (12%), HOMO->L+10 (28%)
96	213.7	0.0004	H-14->L+1 (27%), H-14->L+2 (30%)
97	213.6	0.2204	H-15->L+1 (15%), H-15->L+2 (15%), H-14->L+3 (10%), H-6->L+2 (12%), H-5->L+4 (10%)
98	212.3	0.0384	H-7->L+3 (79%)
99	212.2	0.0187	H-6->L+3 (86%)
100	212.2	0	H-10->L+1 (14%), H-10->L+2 (47%)

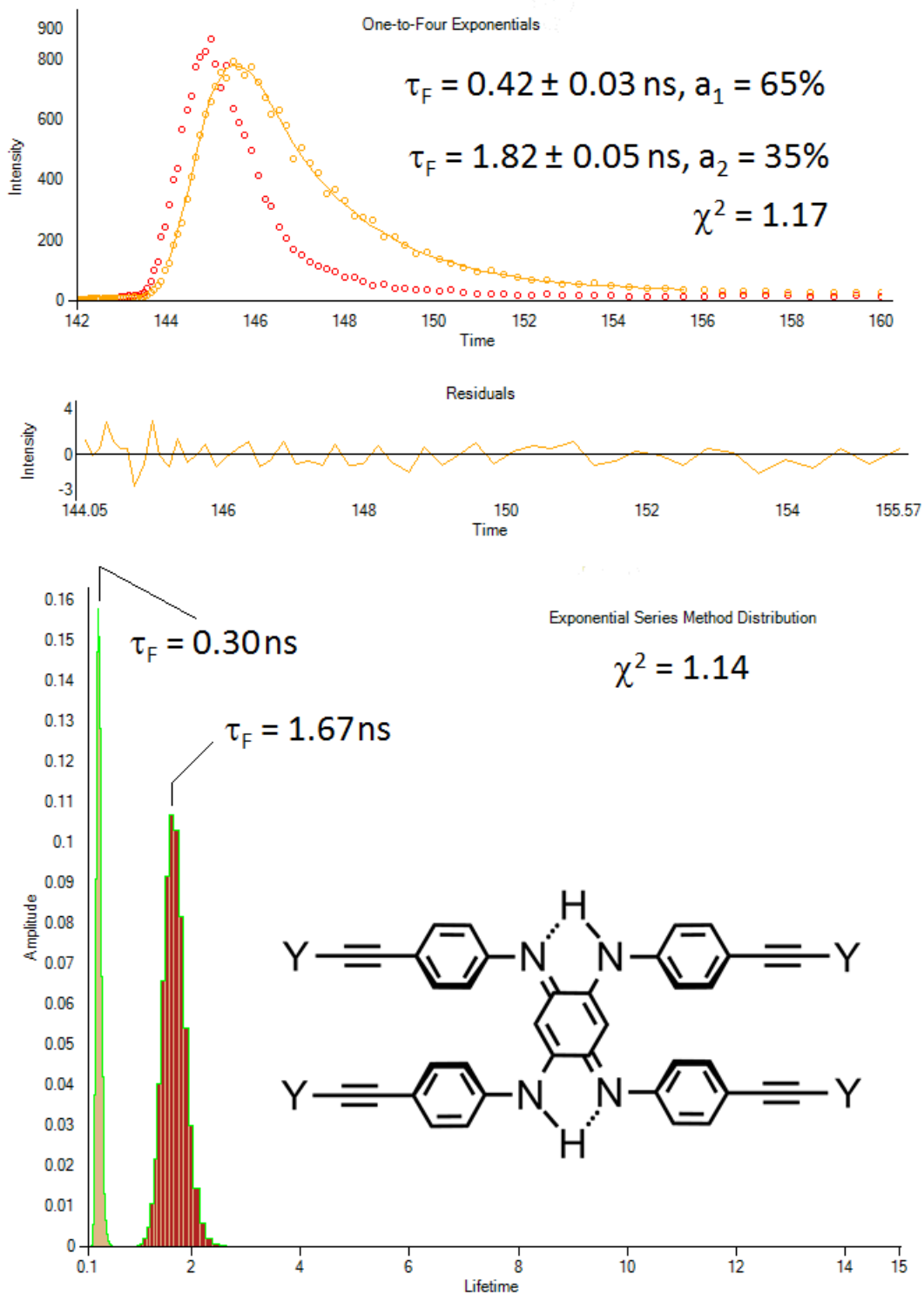


Fig. S18. Top: Fluorescence decay of **1** in 2MeTHF at 77K ($\lambda_{\text{em}} = 750 \text{ nm}$; yellow points), lamp profile (red points), and curve fit (yellow line) analysed using a double exponential fit. Middle: residual. Bottom: ESM analysis of the decay curve ($\text{Y} = \text{SiMe}_3$).

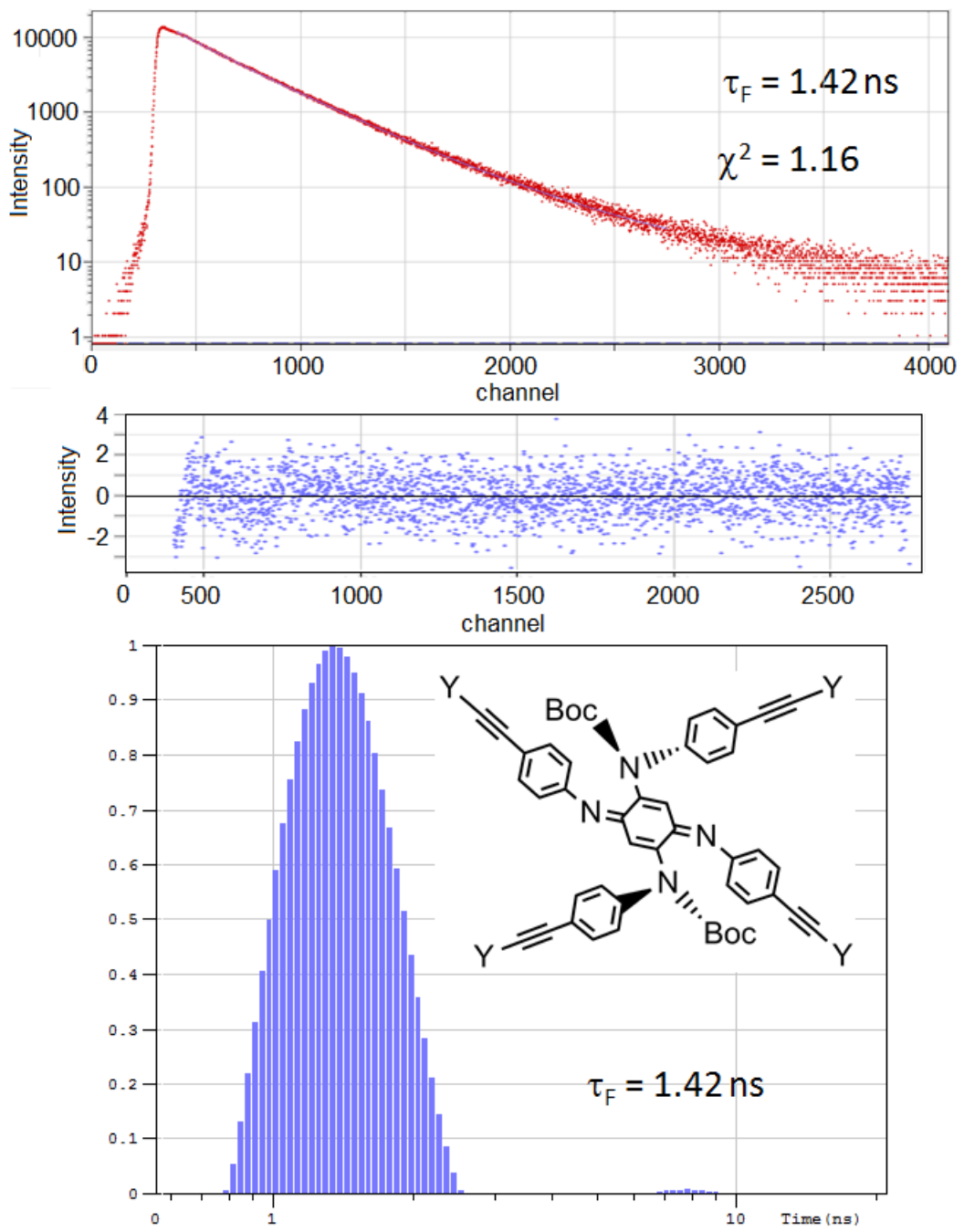


Fig. S19. Top: Fluorescence decay of **2** in 2MeTHF at 77K ($\lambda_{\text{em}} = 385 \text{ nm}$; red points), and curve fit (blue line) analysed using the ESM. The lamp profile is not shown ($\lambda_{\text{exc}} = 375 \text{ nm}$; FWHM = 90 ps). Middle: residual. Bottom: ESM analysis of the decay curve (Y = SiMe₃).

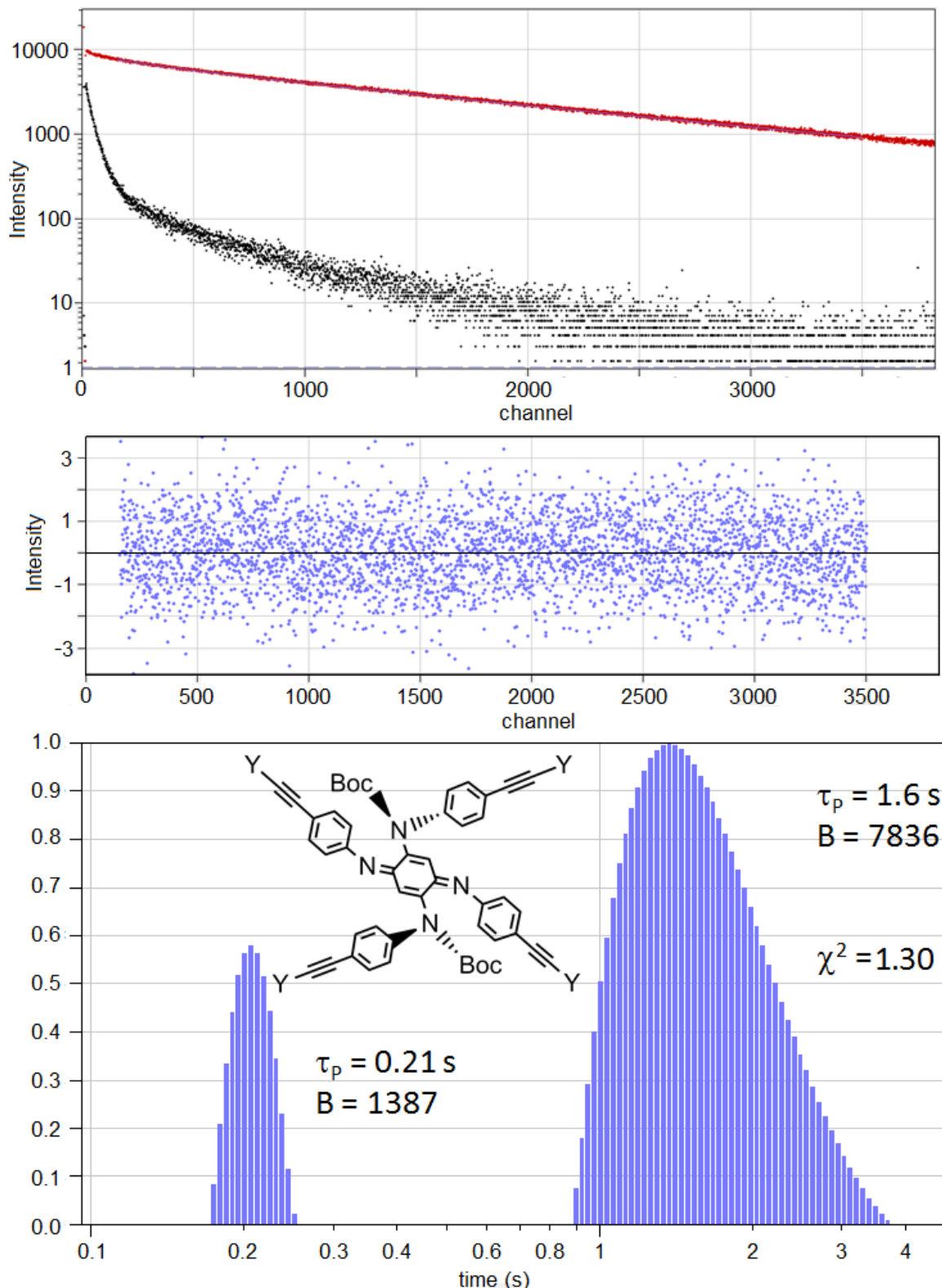


Fig. S20. Top: Phosphorescence decay of 2 in 2MeTHF at 77K ($\lambda_{\text{em}} = 455\text{ nm}$; red points), lamp profile (black; $\lambda_{\text{exc}} = 375\text{ nm}$; FWHM = $\sim 2\text{ }\mu\text{s}$) analysed using the ESM. Middle: residual. Bottom: ESM analysis of the decay curve (Y = SiMe₃).